Columbia University
in the City of New York

DEPARTMENT OF CIVIL ENGINEERING
AND ENGINEERING MECHANICS

INFLUENCE DIAGRAMS FOR STRESSES AND DISPLACEMENTS
IN A TWO-LAYER PAVEMENT SYSTEM
FOR AIRFIELDS

PART I

by

Donald M. Burmister

Columbia University
in the City of New York

DEPARTMENT OF CIVIL ENGINEERING
AND ENGINEERING MECHANICS

INFLUENCE DIAGRAMS FOR STRESSES AND DISPLACEMENTS

IN A TWO-LAYER PAVEMENT SYSTEM

FOR AIRFIELDS

PART I

by

Donald M. Burmister

DEPARTMENT of the NAVY

BUREAU of YARDS and DOCKS

WASHINGTON 25, D. C.

Contract NBy 13009

Technical Report No. 1

JANUARY 1955

ABSTRACT
PART I

PART I presents Influence Diagrams for Stresses and Deflections in Two-Layer Pavement Systems for Airfields, which are intended to provide the essential background and bases for understanding the character and effectiveness of layered system reinforcing action. Influence diagrams of vertical stresses and shear stresses at intervals of depth in layered systems and deflections at the surface are presented covering suitable ranges of the basic two-layer system parameters. The significance of these influence diagrams are discussed with regard to the character and effectiveness of two layer system reinforcing and to their interacting influences on pavement system performances under wheel loads. The major objectives are to develop a "feeling", intuition, and judgment regarding the nature of vertical stress, shear stress, deflection, and shear deformation phenomena and performances, as essential bases for developing relationships and criteria for design of multi-layer pavement systems.

SUBSEQUENT PARTS

PART II will present Influence Diagrams for Stresses and Deflections in Three-Layer Pavement Systems, in order to provide the essential background and bases for understanding the character and effectiveness of three layer system reinforcing action and stress-deflection performances.

PART III will present and illustrate methods and procedures - (1) stresses and deflections in two and three layer systems for any type of wheel loading; (2) for evaluation of their character, magnitude, and significances in critical regions; (3) for improving pavement performances and (4) for providing essential information, which are intended to lead to the formulation of significant design relationships and criteria for multi-layer pavement systems in order to ensure permanence, integrity, and long life of multi-layer pavement structures.

TABLE OF CONTENTS
PART I

INFLUENCE DIAGRAMS
FOR STRESSES AND DISPLACEMENTS
IN TWO-LAYER PAVEMENT SYSTEMS
FOR AIRFIELDS

The work under Phase I of Computations of Stresses and Displacements in a Two-Layer Pavement System was undertaken in the Department of Civil Engineering during the period from April 15, 1957 to September 23, 1959 under Contract NBy-13009 of the Department of The Navy, Bureau of Yards and Docks, Washington 25, D. C., with Columbia University, New York, N.Y., 10027. The programming of stresses and displacements in the Two-Layer System was done under Sub Contract I by Computer Usage Company, Incorporated, 18 East 41st Street New York, N.Y., 10017. The numerical values of stresses and displacements were computed on the IBM 704 at Eglin Air Force Base, Florida, by Computer Usage Company. Incorporated, 655 Madison Avenue, New York, N.Y., 10021. The computing machine time was furnished by the United States Air Force under this contract agreement.

STRESSES AND DEFLECTIONS IN A TWO-LAYER
PAVEMENT SYSTEM FOR AIRFIELDS

INTRODUCTION

Investigations of the deflections of a pavement system
and of the vertical and shear stresses imposed in the support-
ing layers by wheel loads of aircrafts are essential aspects
of pavements studies and design. An airfield pavement is a
preconditioned and prestressed layered system and performs as
an integral structural unit. The performances of a pavement
system under wheel loads are predetermined not only by the
strength properties incorporated in the component layers of
selected materials by construction procedures and sequences,
but also by the confining and restraining influences of each
layer on the other layers of the pavement system and by the
shear continuity within and between the layers established by
construction methods and sequences.

The fundamental performance characteristics of two-layer
pavement systems are treated in order to provide the essential
background and bases for understanding and judgments regard-
ing the character and effectiveness: (1) of the load spread-
ing capacity; (2) of the stress reducing influences of the
pavement reinforcing layers on the vertical stresses imposed
in the supporting subgrade soils; and (3) of the capacity of
a layered pavement system to resist shear and tensile stresses
in regions which are vulnerable to breakdown by shear deforma-
tions and bending.

The principal problems of design and construction of lay-
ered pavement systems are; (1) to limit accumulated permanent

settlements under repeated wheel loads to non-objectionable values; (2) to ensure the permanence and integrity of the pavement structure against shear failure, cracking and break-down; and (3) to increase the life of a pavement structure, giving due consideration to scientific, practical, and economic aspects. The design of multi-layer pavement systems adequately to satisfy these fundamental requirements involves: (1) the determination of the number of layers required; (2) the selection of suitable high quality layer materials and the determination of representative layer shear and tensile strengths and layer modulii; and (3) the evaluation of the thickness requirements for these layers.

Two and three layer system problems presented in 1943 [1] and 1945 [2] (numbers in breackets refer to a list of references) represent a closer agreement with actual stress and deflection performances of layered pavement systems. They provide fundamental parametric relations and equations of physical laws that govern layered system performances. A basic understanding of layered system action and correct conceptions regarding stress-deflection responses, reinforcing action and load spreading capacity, and shear deformation and bending characteristic are essential, as a first prerequisite.

It should be realized at the outset that the problems of design and construction of layered pavement systems deal with the responses of imperfectly elastic materials. It is granted in the present state of knowledge that theory represents an imperfect working hypothesis, which should not be accepted and used at "face value", but must be used with discretion, "common sense", and judgment in the light of experience. A working hypothesis, imperfect though it may be, is indispens-able, because - (1) it can increase understanding and knowl-edge of observed phenomena, (2) can tell the investigator what

quantities and parameters must be observed and measured, (3) can enable the investigator more completely and correctly to interpret and evaluate the results of observations and experiences through significant and fundamental parametric relations, which reveal the complex interacting influences of these quantities and parameters.

Furthermore, it must be realized in applying imperfect physical laws and theories to layered pavement systems, that evaluation and design are more of the nature of an ART than a science in the present state of knowledge. The practice of an ART requires a broad background of fundamental knowledge, a wide practical experience, a capacity to visualize, interpret and evaluate correctly situations with regard to the conditions that control, and a high order of common sense, judgment, and a sense of responsibility. The major problem confronting engineers in the design of layered pavement systems are those of learning how effectively and reliably to work with and to use an imperfect theory and to eliminate the guess work in judgment: (1) by thoroughly and competently testing theory against observed and measured performances, comparing what was expected with what really happened, and evaluating the reasons for discrepancies; (2) by comprehending the limitations of theory and establishing the reasonable realm of validity within which one can work with some confidence; and (3) by evaluating and reliably establishing the regions in and the degree to which real soils, real pavement materials, and real field conditions may be expected to agree with or to depart from the idealized conditions of the imperfect theory, particularly with regard to stress-deflection and shear-deformation responses of layered systems. Thus one can learn how to build, up, fortify and justify one's judgment in making final design decisions. It is evident that the use and applications of

an imperfect theory should never be allowed to become merely a routine, superficial, and unimaginative matter. A high professional status of this ART of layered pavement design should be the true objective with an acceptance of responsibility for adequacy of design judgments.

To many engineers it seems difficult to understand and to reconcile the many different practices and the divergence of opinions in highway and airfield pavement designs. But in reality this situation should be accepted as the expected usual working conditions, where great differences actually exist in different regions with regard to soil character, geological processes of formation of soil deposits, prevailing climatic conditions and environmental influences, ground slopes and ground water conditions, stratification of soil deposits, prestress history, and construction and service conditions [7 to 22]. It should be realized that pavements are constructed and used in the surface zones of greatest exposure to environmental influences, whether at natural ground surface in excavations, or in embankments. Furthermore, the original prevailing environmental influences are always modified by construction methods and sequences and by the pavement itself. The importance and controlling influences of these environmental conditions have been treated in a series of ASTM papers, presenting the concepts and principles of the environmental approach [7 to 22].

Although the environmental conditions with regard to scope, character and influences may be expected to vary widely in different regions of the United States, yet in the local region of each person's experience and work, valid opinions and practices may be developed to "fit" the specific prevailing soil and environmental conditions. It should be realized,

however, that these opinions and practices can not be transplanted and can not be expected to be valid in other regions having appreciably different prevailing soil and environmental conditions. In local areas of each person's experiences and practices, it is possible to establish, understand. and effectively deal with: (1) the character and range of prevailing environmental influences; (2) the kind, relative dominance, and degree of control; (3) the favorable and adverse influences; (4) how and to what degree these influences are modified and changed by construction methods and sequences; and (5) how and to what degree conditions can be permanently improved by advance planning, processing of materials, and special construction treatments. These are major aspects of pavement design and construction, which require thorough investigations, evaluations, and specific and correct solutions in each particular situation. A general favorable average of conditions in a region may serve as a reference design basis, but modifications of this reference design basis must specifically be made in order to take into account adequately, practically, and economically the degree of importance or severity of controlling unfavorable or adverse environmental, constructional. and service conditions.

Therefore it would be unrealistic and misleading to suppose that all a stress investigation demands is merely facility in the use of stress influence charts and stress performance ratings. Present thinking and practices tend to be too matter-of-fact and unimaginative without giving thought and study to the realm of validity of stress investigations, to the influences of geological, environmental, and structure conditions that control, and to the adequacy and reliability of the results of stress investigations. There is an essential need for a realistic, mature, and common sense approach and engi-

neering imagination in making stress investigations. The ma-
jor objectives are: (1) to develop judgment and a "feeling"
regarding the real nature of stress and displacement phenomena
in soil; (2) to remove "ignorance factors and guess work" from
stress investigations. Stress investigations must be capable
of development and growth to meet the demands for specialized
and complex studies of stress and displacement conditions in-
volved in the design and construction of airfield pavements.
Thus the estimated stress and displacement conditions can be
brought into closer agreement with the actual stress and dis-
placement conditions imposed by airfield pavement loadings.
A major aspect is to raise the standards of excellence in
practices and the conceptions of adequacy and reliability.

CONCEPTS AND PRINCIPLES

Certain concepts and principles regarding pavement performances and influences of environmental and service conditions are of fundamental importance in understanding and dealing with layered pavement systems (Indicated by "C" numbers, as C1, C2, etc.) [5, 6, 7, 21]. Stresses and displacements estimated by two and three layer problems [1, 2] represent a closer agreement with actual stress and deflection performances of layered pavements systems. In general, design always deals with multi-layer pavement systems, which should be "fitted" by design to actual environmental and service conditions.

C1 - An airfield pavement is inherently a preconditioned and prestressed layered system, which is constructed "in-place" and performs as an integral structural unit. C2 - The subgrade in excavation and in embankment is prepared and preconditioned by systematic heavy rolling to incorporate by compaction definite density and strength properties, and of equal importance is prestressed to pressure intensities greater than the stresses anticipated under service conditions.

In sequence a subbase layer is placed on this subgrade and is likewise preconditioned and prestressed by heavy rolling. C3 - The subgrade layer is now importantly and effectively confined and restrained at subgrade interface by the physical weight and stiffness of this compacted subbase layer and is still further prestressed in this confined condition due to restrained rebound effects. C4 - Even more important and effective is the shear strength continuity and mechanical bond thus incorporated under these restrained conditions.

The placing and compacting in sequence of a base course layer and an asphalt pavement layer (or concrete pavement layer) increases the degree and effectiveness of the prestress, restraints, and shear strength continuity at the layer interfaces and throughout the layers. C5 - Thus finally the layered pavement is incorporated into an integral prestressed structure composed, in reality, of new materials having greatly improved strength and performance properties. Although greater densities may be attained in granular materials by vibratory equipment alone, still the most essential aspect of construction is the prestressing, keying of aggregates. and shear strength continuity attained by systematic heavy rolling sequences.

C6 - Only materials of the subgrade - pavement structure. which possess appreciable internal friction, are capable and competent to maintain for the anticipated life of a pavement structure, the prestress, restraint and confinement conditions, and shear strength continuity without relaxation to a premature failure under repeated load applications. C7 - The natural environmental conditions, particularly with regard to changes in moisture content and to frost action, are modified importantly by construction conditions of a pavement system and by imposed service conditions, and they have controlling influences on the strength and deflection responses of the subgrade soils and hence on the performances and life of layered pavement systems.

TWO LAYER SYSTEM CONDITIONS AND PARAMETERS

A multi-layer pavement system is illustrated in Fig. 1(a), which is composed of reinforcing layers - asphalt pavement course, base course, subbase, and compacted subgrade, and of a subgrade layer. The strength properties, such as the modulii, E and Poisson's ratio, μ, and the thicknesses, h of the layers are indicated. Under Phase I a two layer system is treated, as illustrated in Fig. 1(b). The two layer system is composed of an homogeneous reinforcing layer 1 having strength properties, E_1 and μ_1 and thickness, h_1, and a subgrade layer 2 of infinite thickness having strength properties, E_2 and μ_2. The multi-layer pavement system of Fig. 1(a) may be treated, as discussed later, as a two layer system composed of an homogeneous reinforcing layer 1 equivalent in effective strength properties and thickness to the combined reinforcing asphalt, base course subbase, and compacted subgrade layers, and of the same subgrade layer 2.

The usual boundary conditions of the theory of elasticity for a semi-infinite mass loaded at the surface apply here. The surface at z = 0 is free of vertical and shear stresses outside the load limits. At z and r equal to infinity all stresses and displacements become equal to zero. The layers of the layered system within themselves are composed of homogeneous, isotropic materials. The conditions of equilibrium of stresses and of compatibility of strains are satisfied in each layer of the layered system. In addition, four continuity conditions of Eq. 1 for a two layer system are satisfied across the interface 1-2 between reinforcing layer 1 and subgrade layer 2 in order to insure continuity of transmission of stresses and

strains across this interface. This means that the two layers
work together as a structural unit without any slippages or
loss of contact between the layers. There is, however, a dis-
continuity in the radial stress, σ_r across interface 1-2,
because v'th horizontal displacements, $u_1 = u_2$ in Eq. (1),
the magnitudes of the radial stresses, σ_{r1} and σ_{r2} on either
side of the interface must necessarily be determined by the
respective modulii, E_1 and E_2 of layers 1 and 2.

The two layer stress and displacement equations in layers
1 and 2, for which influence values have been computed under
this contract, are given as follows: vertical stress, σ_z in
Eqs. (5); shear stresses, τ_{rz} in Eqs. (6); and vertical de-
flections or settlements, w in Eqs. (7). In addition for
future reference, there are given: horizontal stresses, σ_r
and σ_θ in Eq. (8) and Eq. (9); shear stresses $\tau_{r\theta}$ in Eq. (10);
and horizontal displacements, u in Eq. (11), for which the nu-
merator brackets are given in Eqs. (12) to (15). The two layer
denominator, D, which is common to all stress and displacement
equations, is given in Eq. (4).

The two layer stress and displacement Eqs. (4) to (15)
reveal the dependence of stresses and deflections upon the two
layer strength ratios, n, M, and L of Eq. (3). The computa-
tions of stresses and deflections cover the range of Poisson's
ratio, μ and of the modulii ratio, E_1/E_2 indicated under
Eq. (3). In order to facilitate the computations of stresses
and deflections, the depth-thickness ratio, z/h is referenced
in Fig. 1(b) to $z' = 0$ at interface 1-2 throught the subsidiary
relations: $z' = -ch$ for layer 1 and $z' = +dh$ for layer 2.
The true depths in the two layer system for tabulations of the
computed stress and deflection influence values are referenced
to $z = 0$ at the top surface of layer 1 by the relations: $z = (1-c)h$

Multi-Layer Pavement System

Layered System Continuity Conditions Eq. (1) at Interface 1 - 2 between Reinforcing Layers 1 and Subgrade Layer 2.

$$\leftarrow 2\ r_o \rightarrow$$

$z = 0$

Bearing Pressure, P

h_p Asphalt Layer E_p μ_p

h_b Base Course Layer E_b μ_b

h_{sb} Subbase Layer E_{sb} μ_{cb}

$$\sigma_{z1} = \sigma_{z2}$$

$$\tau_{rz1} \quad \tau_{rz2}$$

Displacements $\quad w_1 = w_2$

$$\mu_1 = \mu_2$$

Basic Layered System Parameters - Eq. (2)

Modulii Strength Ratio - E_1/E_2

h_{cs} Compacted Subgrade E_{cs} μ_{cs}
Layer

Interface1 - 2

$z = h_1$

Subgrade Layer 2 E_s μ_s

Ratio of Radial Distance - r/h to Thickness of Layer 1.

Ratio of Vertical Distances to z/h Thickness of Layer 1.

Integration Parameter $\lambda = mh$

a)   Typical Multi-Layer

$$\leftarrow 2\ r_o \rightarrow$$

For Computations.   For Data and Curves.

$c = 1.0$ $z' = -h$ $z = 0$

$c = 0.5$ $z = + (1-c)h$

$c = 0$
$d = 0$ $z' = 0$ $z = h$

$d = 0.5$ $z = + (1+d)h$

$d = 1.0$ $z' = +h$ $z = 2h$

b)   Two Layer System. Depth Parameters for Computations.
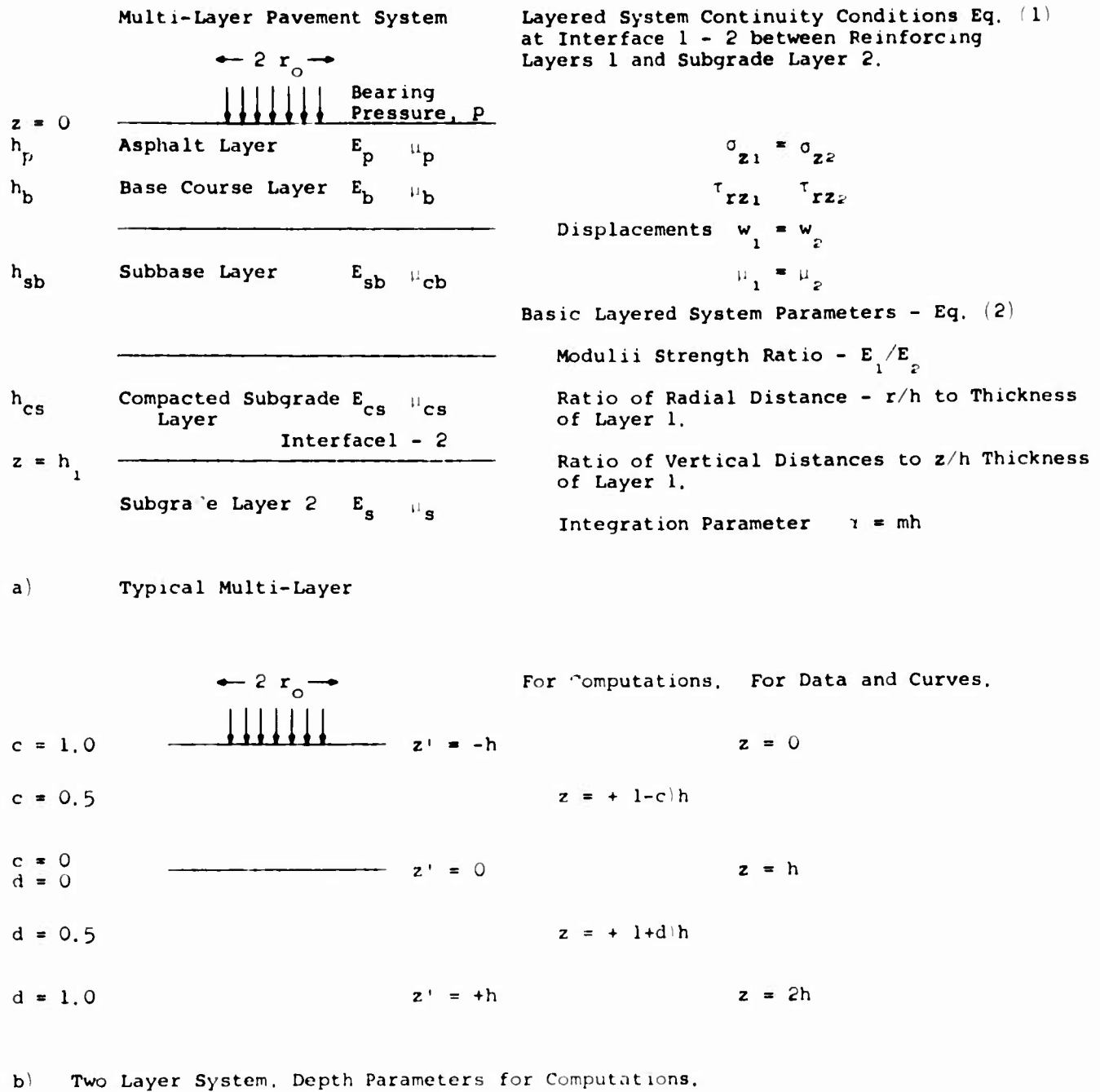
FIG. 1   LAYERED SYSTEM NOTATIONS, BASIC CONTINUITY CONDITIONS, AND BASIC LAYERED SYSTEM PARAMETERS.

for layer 1, and $z = (1 + d)h$ for layer 2 in Fig. 1 (b). The stress and deflection Eqs. (4) to (15) now reveal the dependence of stresses and deflections upon the fundamental two layer parameters: r/h, z/h, and E_1/E_2 of Eq. (2) and Fig. 1(b), and the integration parameter, α.

The following ranges and intervals of the layered system parameters were covered by systematic steps in the computations of stress and deflection influence values.

Table A - <u>Range of Two Layer System Parameters in Fig. 1</u>

r/h- 0 to 1.0 at intervals of $(\Delta r)/h$-0.02(50 values)

1.0 to 5.0 at intervals of $(\Delta r)/h$-0.10(50 values)

5.0 to 25.0 at intervals of $(\Delta r)/h$-0.50(40 values)

$z'= -ch$ in layer 1; σ_z - $c = 0, 0.5$ $d = 0.5, 1, 2,$ and 4
$z'= +dh$ in layer 2

τ_{rz}- $c = 0, 0.5$ $d = 0.5, 1, 2,$ and 4

w - $c = 0, 1.0$

Range of μ	(1)	(2)	(3)	(4)
μ_1	0.2	0.4	0.2	0.4
μ_2	0.2	0.2	0.4	0.4

Range of E_1/E_2 1, 5, 10, 20, 50, 100, 200, 500, 1000, 2000, 5000, 10000, 20000, 50000.

TWO LAYER PAVEMENT SYSTEM EQUATIONS

Two Layer Strength Ratios

$$n = \frac{E_2}{E_1}\frac{1+\mu_1}{1+\mu_2} \qquad M = \frac{1-n}{1+(3-4\mu_1)n} \qquad L = \frac{(3-4\mu_2)-(3-4\mu_1)n}{(3-4\mu_2)+n} \qquad (3)$$

	(1)	(2)	(3)	(4)
Range of μ_1 =	0.2	0.4	0.2	0.4
μ_2 =	0.2	0.2	0.4	0.4

Range of E_1/E_2 for each combination of (μ_1, μ_2) in Table A.

Two Layer Denominator, D.
Common to all stress and displacement equations for the two layer system.

$$D = [1 - (L+M)E^{-2\alpha} - 4M\alpha^2 e^{-2\alpha} + L\,M\,e^{-4\alpha}] \qquad (4)$$

Stress and Deflection Equations.
Beneath the center of a uniformly loaded circular area for which influence values have been computed.

$$\text{Vertical Stress} - \sigma_z = p\left[\frac{\theta}{2\pi}\right]\int_0^\infty \frac{[N-1]}{D}\frac{r}{h}J_1(r\alpha/h)\,d\alpha \qquad (5)$$

Layer 1 σ_{z1}

$$[N-1]_1 = \;+\,e^{-(1-c)\alpha} + (1-c)\alpha e^{-(1-c)\alpha} \qquad (5a)$$
$$-\,0.5(L+M)e^{-(1+c)\alpha} - M(1+c)\alpha e^{-(1+c)\alpha} - 2Mc\alpha^2 e^{-(1+c)\alpha}$$
$$-\,0.5(L+M)e^{-(3-c)\alpha} + M(1+c)\alpha e^{-(3-c)\alpha} - 2Mc\alpha^2 e^{-(3-c)\alpha}$$
$$+\,L\,M\,e^{-(3+c)\alpha} - L\,M(1-c)\alpha e^{-(3+c)\alpha}$$

Layer 2 σ_{z2}

$$[N\ 1] = \quad + e^{-(1+d)\alpha} + (1+d)\alpha e^{-(1+d)\alpha} \tag{5b}$$

$$- 0.5(L+M)e^{-(1+d)\alpha} - (Ld+M)\alpha e^{-(1+d)\alpha}$$

$$- 0.5(L+M)e^{-(3+d)\alpha} + M(1-d)\alpha e^{-(3+d)\alpha} + 2M\ d\alpha^2 e^{-(3+d)\alpha}$$

$$+ L\ M\ e^{-(3+d)} - L\ M(1-d)\alpha e^{-(3+d)\alpha} - 2\ L\ M\ d\alpha^2 e^{-(3+d)\alpha}$$

Shear Stress- $\quad \tau_{zx} = -p[\sin\theta] \int_0^r \frac{rdr}{2\pi} \int_0^\infty \frac{[N\ 6]}{D} \frac{1}{h^2} \frac{J_1(r\alpha/h)d\alpha}{}$

$$\tag{6}$$

$$\tau_{zy} = -p[1-\cos\theta] \times [\text{Same Integrals}]$$

Note- Integrations $\int_0^r rdr$ performed by computational methods.

Angle, θ covers one quadrant only from $0°$ to $90°$, for use in the circular diagram method of integration for any size and shape of loaded area.

Layer 1 τ_{zx1} and τ_{zy1}

$$[N\ 6]_1 = + (1-c)\alpha e^{-(1-c)\alpha} \tag{6a}$$

$$+ 0.5(L-M)e^{-(1+c)\alpha} - M(1-c)\alpha e^{-(1+c)\alpha} + 2M\ c\alpha^2 e^{-(1+c)\alpha}$$

$$- 0.5(L-M)e^{-(3-c)\alpha} - M(1-c)\alpha e^{-(3-c)\alpha} - 2M\ c\alpha^2 e^{-(3-c)\alpha}$$

$$+ L\ M(1-c)\ \alpha e^{-(3+c)\alpha}$$

Layer 2 τ_{zx2} and τ_{zy2}

$$[N\ 6]_2 = + (1+d)\alpha e^{-(1+d)\alpha} \tag{6b}$$

$$+ 0.5(L-M)e^{-(1+d)\alpha} - (Ld+M)\alpha e^{-(1+d)\alpha}$$

$$- 0.5(L-M)e^{-(3+d)\alpha} - M(1+d)\alpha e^{-(3+d)\alpha} + 2M\ d\alpha^2 e^{-(3+d)\alpha}$$

$$+ L\ M(1+d)\alpha e^{-(3+d)\alpha} - 2L\ M\ d\alpha^2 e^{-(3+d)\alpha}$$

Deflection $- w = +2 \left[\dfrac{\theta}{2\pi}\right] \dfrac{pr}{E_2} \int_0^\infty \dfrac{1+\mu_1}{2} \dfrac{E_2}{E_1} \dfrac{[N2]}{D} \dfrac{1}{\alpha} J_1(r\alpha/h) d\alpha$ (7)

$$= 2 \, c \, p \, r \, F_w / E_2$$

Layer 1   w at Surface, $z = 0$ (c=1)

$[N2]_1 = \quad + 2(1-\mu_1)[1+4M\alpha^2 e^{-2\alpha} - L\,M\,e^{-4\alpha}]$ (7a)

Layer 2   w at Interface 1-2, $z = h$ (c = 0)   (7b)

$[N2]_2 = \quad + 2(1-\mu_1)e^{-\alpha} + \alpha e^{-\alpha}$

$\qquad\qquad + 0.5[L + (3-4\mu_1)M]e^{-\alpha} + (3-4\mu_1)M\,\alpha e^{-\alpha}$

$\qquad\qquad - 0.5[L + (3-4\mu_1)M]e^{-3\alpha} + (3-4\mu_1)M\,\alpha e^{-3\alpha}$

$\qquad\qquad - 2(1-\mu_1)L\,M\,e^{-3\alpha} + L\,M\,\alpha e^{-3\alpha}$.

The following additional additional stress and displacement equations are given in order to have a complete set of two layer equations for reference   The integrations, $\int_0^r r\,dr$ are to be made by computational methods. The angle θ in these equations covers one quadrant only from 0° to 90° for circular diagram methods of evaluation for any shape, size, and position of loaded area,

Horizontal Stress, $\sigma_x =$

$-\dfrac{p}{2\pi h^2} \int_0^\infty d\alpha \int_0^r r\,dr \int_0^\theta \left[\dfrac{[N3]}{D} \, \alpha J_0(r\alpha/h) - \dfrac{[N3]}{D} \dfrac{h}{r} J_1(r\alpha/h) + \right.$ (8)

$\qquad \left. \dfrac{[N4]}{D} \alpha J_0(r\alpha/h)\right]_1 \cos^2\theta \, d\theta + \left[\dfrac{[N3]}{D} \dfrac{h}{r} J_1(r\alpha/h)\right.$

$\qquad \left. + \dfrac{[N4]}{D} \alpha J_0(r\alpha/h)\right]_2 \sin^2\theta\,d\theta$

Horizontal Stress, $\sigma_y =$ (9)

$-\dfrac{p}{2\pi h^2} \int_0^\infty d\alpha \int_0^r r\,dr \int_0^\theta [Ditto]_1 \sin^2\theta \, d\theta + [Ditto]_2 \cos^2\theta \, d\theta$

Shear Stress, $\tau_{xy} = \tau_{yx}$ (10)

$$- \frac{p}{2\pi h^2} \int_0^\infty d\alpha \int_0^r r dr \int_0^\theta \left[\frac{[N\ 3]}{D} \alpha\ J_0(r\alpha/h) - 2\ \frac{[N\ 3]}{D}\ \frac{h}{r}\ J_1(r\alpha/h) \right] \times \sin\theta\cos d\theta$$

Horizontal Displacement, u (11)

$$- \frac{p}{2\pi h^2} \int_0^\theta d\alpha \int_0^r r dr \int_0^\infty \frac{[N\ 3]}{D}\ J_1(r\alpha/h) d\alpha$$

Layer 1

$$[N\ 3]_1 \quad + [1-2\mu_1 - (1-c)\alpha]e^{-(1-c)\alpha}$$

$$+ 0.5[L-M\ (3-4\mu_1 - 2c\alpha)(1+2\alpha)]e^{-(1+c)\alpha} \quad (12)$$

$$+ 0.5[L-M\ (3-4\mu_1 + 2c\alpha)\ (1-2\alpha)]e^{-(3-c)\alpha}$$

$$+ L\ M[1-2\mu_1 + (1-c)\alpha]e^{-(3+c)\alpha}$$

$$[N\ 4]_1 \quad + 2\mu_1 e^{-(1-c)\alpha}$$

$$- 2\mu_1 M(1+2\alpha)e^{-(1+c)\alpha} \quad (13)$$

$$- 2\mu_1 M(1-2\alpha)e^{-(3-c)\alpha}$$

$$+ 2\mu_1 L\ M\ e^{-(3+c)\alpha}$$

Layer 2

$$[N\ 3]_2 \quad + [1-2\mu_2 - \alpha(1+d)]e^{-(1+d)\alpha}$$

$$- 0.5[L(3-4\mu_2-2d\alpha - M(1+2\alpha)]e^{-(1+d)\alpha} \quad (14)$$

$$+ 0.5[L-M(3-4\mu_2 - 2d\alpha)(1-2\alpha)]e^{-(3+d)\alpha}$$

$$+ L\ M[1-2\mu_2-(1+d)\alpha - 2\alpha(1-2\mu_2 - d\alpha)]e^{-(3+d)\alpha}$$

$$[N\ 4]_2 \quad + 2\mu_2 e^{-(1+d)\alpha}$$

$$- 2\ L\ \mu_2 e^{-(1+d)\alpha} \quad (15)$$

$$- 2\ M\ \mu_2(1-2\alpha)e^{-(3+d)\alpha}$$

$$+ 2\ L\ M\ \mu_2(1-2\alpha)e^{-(3+d)\alpha} \quad .$$

CHARACTER OF TWO LAYER SYSTEM EQUATIONS

Two layer system performances, with regard to stress transmission characteristics, and magnitude and distribution of stresses imposed in the layers by surface loads, are governed by the complex interacting influences of the fundamental two layer parameters of Eq. (2): (1) the effective modulii ratio, E_1/E_2 in Eq. (3) of the relative strength properties incorporated by construction in the reinforcing layer 1 and subgrade layer 2, which is to be protected; (2) the ratio, r/h of the radius of the bearing area or tire contact area to the thickness of reinforcing layer 1; and (3) the ratio, z/h of the depths in the layered system to thickness of reinforcing layer 1. The deflection performances of a two layer system with regard to reinforcing action, stiffness, and load spreading capacity of layer 1, are governed by the settlement coefficient, F_w of Eq. (7), which by the parametric relation, $F_w[E_1/E_2, \mu_1, \mu_2, r/h, z/h]$ expresses not only the controlling interacting influences of all these parameters, but also the influences of the preconditioning and prestressing of the layered system and of the restraints and shear strength continuity incorporated in the layer interface and throughout layer 1.

The stress and deflection equations reveal by their parametric relations the dependence of stresses and deflections upon the fundamental two layer parameters of Eqs. (1) to (3). They also reveal by the systematic form of the four lines of each equation, the fundamental nature of the physical parametric relations of Eqs. (4) to (15) that exist among the two layer parameters which govern stress and deflection performances. The two layer common denominator, D of Eq. (4) insures the continuity

of stresses and displacements across interface 1-2. The re-
inforcing action, stiffness, load spreading capacity, and stress
reducing capacity of layer 1 on stresses imposed in subgrade
layer 2 are of principal concern in evaluating deflection bend-
ing, and shear-deformation performances of layered systems.
These fundamental performance characteristics of a two layer
system are treated in considerable detail in order to provide
essential bases for understanding, intuitive thinking, evalua-
tion, and judgments regarding their real character and effec-
tiveness over the full range of two layer parameters given
above in Table A and Eq. (3), as follows: vertical stresses
σ_z; shear stresses, τ_{rz}, and vertical deflections, w, for
which computations of influence values have been completed
under this contract.

VERTICAL STRESS INFLUENCE CURVES

$$\sigma_z/p \text{ vs } r/h \text{ and } E_1/E_2$$

Thorough knowledge and understanding of, and clear insight into the fundamental stress transmission characteristics and stress performances of two layer systems are essential for air-field pavement studies, evaluations, and designs. The character, magnitude, and distribution of vertical stresses, σ_z imposed by wheel loads in layers 1 and 2 of a two layer system are of principal concern- first, because they disclose the effectiveness of reinforcing action and load spreading capacity of a strong reinforcing layer 1 in protecting a relatively weak subgrade layer 2; and second, because they make it possible to delineate regions of possible critical stresses in the different layers and at different locations with respect to single and dual wheel loadings or landing gear loadings applied on a pavement surface.

First of all, a series of general vertical stress performance ratings have been plotted in Figs. 2, 3, 4 and 5 from data computed under this contract. The curves of these figures represent the vertical stress influences imposed at interface 1-2 on the center line beneath a surface loading uniformly distributed over circular areas of increasing radius, $r = [r/h]h$. These figures disclose the nature of vertical stress performances and effectiveness of reinforcing action, as governed by the basic two layer parameters- E_1/E_2, (μ_1, μ_2), r/h and z/h. Vertical stress influence coefficients, σ_z/p at the interface 1-2 for $z/h = 1.0$ are plotted against the parameter, r/h increasing from 0 to 6, forming a systematic family of influence curves for the full range of E_1/E_2, Table A from 1.0 (the

FIG. 2 TWO LAYER VERTICAL STRESS INFLUENCE CURVES

σ_z/p versus r/h

at Interface 1-2, $z = h$

(1) $\mu_1 = 0.2$ $\mu_2 = 0.2$
(2) $\mu_1 = 0.4$ $\mu_2 = 0.2$

Vertical Stress Influence Coefficient, σ_z/p beneath Center of Uniformly Loaded Circular Area

Values of Two Layer Parameter - r/h

E_1/E_2

-21-

FIG. 3 TWO LAYER VERTICAL STRESS INFLUENCE CURVES

σ_z/p versus r/h
at Interface 1-2, $z = h$

——— (3) $\mu_1 = 0.2$ $\mu_2 = 0.4$
——— (4) $\mu_1 = 0.4$ $\mu_2 = 0.4$

Vertical Stress Influence Coefficient, σ_z/p beneath Center of Uniformly Loaded Circular Areas

Values of Two Layer Parameter - r/h

E_1/E_2

FIG. 4 TWO LAYER VERTICAL STRESS INFLUENCE CURVES

σ_z/p versus r/h

at Interface 1-2, $z = h$

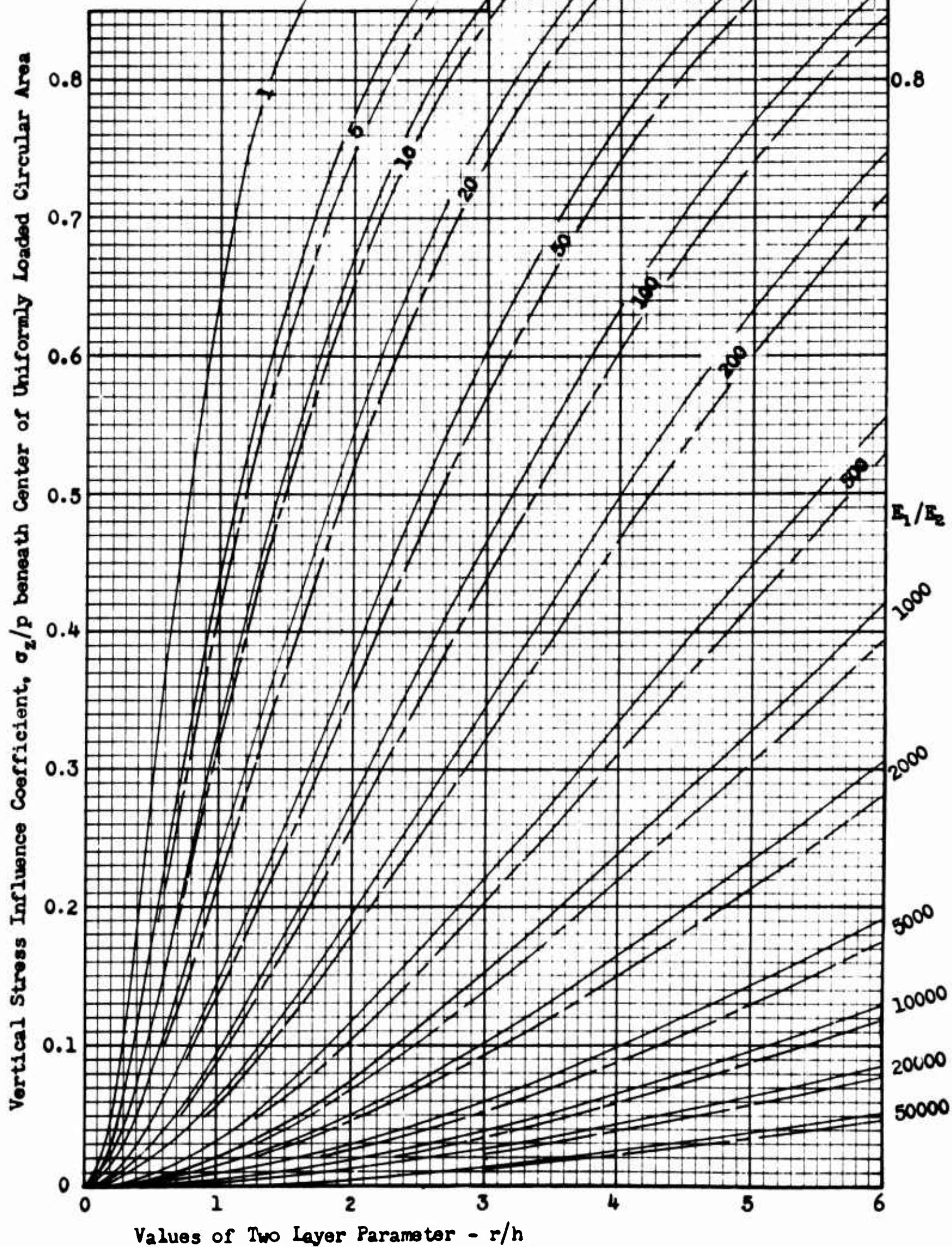(1) $\mu_1 = 0.2$ $\mu_2 = 0.2$

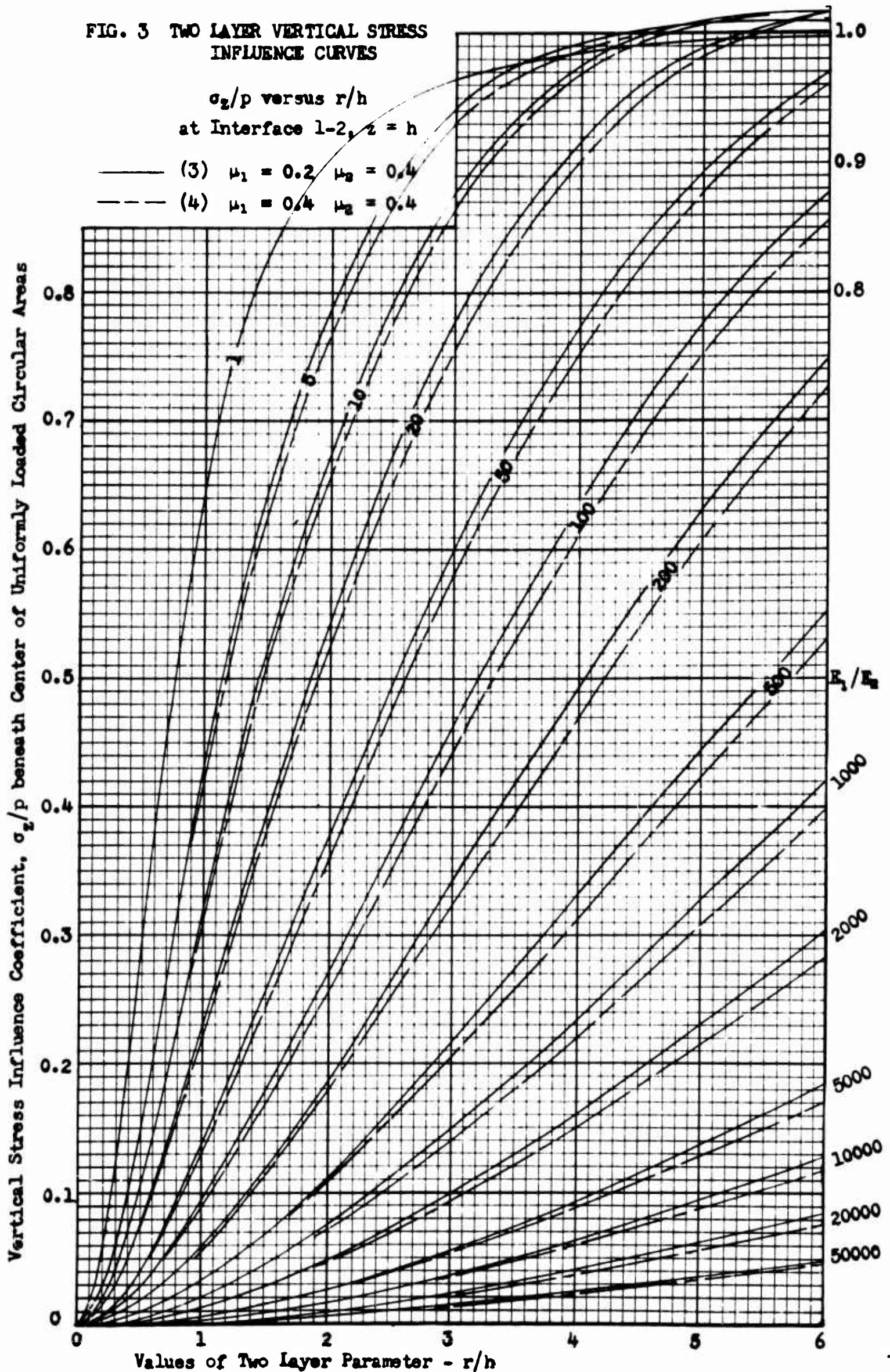(3) $\mu_1 = 0.2$ $\mu_2 = 0.4$

Vertical Stress Influence Coefficient, σ_z/p beneath Center of Uniformly Loaded Circular Areas

Values of Two Layer Parameter - r/h

E_1/E_2

FIG. 5 TWO LAYER VERTICAL STRESS
INFLUENCE CURVES

σ_z/p versus r/h

at Interface 1-2, $z = h$

——— (2) $\mu_1 = 0.4$ $\mu_2 = 0.2$

— — — (4) $\mu_1 = 0.4$ $\mu_2 = 0.4$

Vertical Stress Influence Coefficient, σ_z/p beneath Center of Uniformly Loaded Circular Areas

Values of Two Layer Parameter - r/h

E_1/E_2

Boussinesq case) to 50,000. The values of Poisson's ratio, μ_1 and μ_2 for layers 1 and 2 are held constant for each figure, as noted.

The marked increase in effectiveness of the reinforcing action and load spreading capacity of layer 1 with increase in E_1/E_2 for constant values of the parameter, r/h along vertical lines in Figs. 2 to 5 is disclosed by the marked reduction in the vertical stress influence coefficient, σ_z/p at the top of subgrade layer 2 in interface 1-2. This is illustrated in Table 1 by the decreasing values of σ_z/p in horizontal lines for selected values of r/h. On the other hand there is considerable decrease in effectiveness with increase in r/h along constant E_1/E_2 curves, as illustrated by the increase in σ_z/p in the vertical columns of Table 1.

Table 1. Effectiveness of Reinforcing Action of Two Layer
         Systems in Reducing Vertical Stresses Imposed on
         Subgrade Layer 2, as Indicated by Values of σ_z/p
         at Interface 1-2 versus E_1/E_2 and r/h for $\mu_1 = 0.2$,
         $\mu_2 = 0.4$, in comparison with the Boussinesq Case,
         $E_1/E_2 = 1.0$.

E_1/E_2

r/h	1	5	10	20	50	100	200	500	1000	2000	5000	10,000
0.5	0.284	0.161	0.113	0.076	0.043	0.027	0.017	0.009	0.006	0.004	0.002	0.001
1.0	0.646	0.424	0.310	0.228	0.138	0.092	0.060	0.034	0.021	0.014	0.008	0.005
1.5	0.829	0.634	0.511	0.389	0.253	0.175	0.118	0.069	0.045	0.029	0.016	0.010
2.0	0.911	0.784	0.670	0.540	0.374	0.269	0.188	0.112	0.074	0.049	0.029	0.018

Figures 2, 3, 4 and 5, Table 1, and Eq. (5) show that the effectiveness of reinforcing action and load spreading capacity of reinforcing layer 1 on subgrade layer 2 depend on the two layer parameters, E_1/E_2 and r/h, and pressure, p. Effectiveness is increased: (1) by use of higher strength, E_1/E_2 materials in layer 1 for constant values of h, c, and p; and (2) by an increase in thickness, h of layer 1 for constant E_1/E_2, r, and p.

Equivalent two layer systems with regard to reinforcing action are indicated for constant σ_z/p values on horizontal lines in Figs. 2 to 5 by various E_1/E_2 and r/h combinations in Table 2.

Table 2. Equivalent Two Layer Systems for Constant σ_z/p Values at Interface 1-2 from Fig. 3 for $\mu_1 = 0.2$ and $\mu_2 = 0.4$ Values of r/h for E_1/E_2.

σ_z/p	5	10	20	50	100	200	500	1000
0.5	1.15	1.45	1.85	2.53	3.20	4.05	5.50	6.90
0.2	0.60	0.73	0.91	1.27	1.63	2.08	2.85	3.62
0.1	0.41	0.48	0.58	0.82	1.05	1.35	1.87	2.39

In order to bring out clearly regions of significant influences of Poisson's ratio, μ in layers 1 and 2, combinations have been plotted in Figs. 2 to 5 for direct comparison, and the influences are analyzed in Table 3. Poisson's ratio of 0.2 is considered applicable to granular materials of base courses subbases and subgrades. Poisson's ratio of 0.4 is considered applicable to asphalt pavement courses and clay soil subgrades.

Table 3. Regions of Significant Influences of Poisson's Ratio, μ_1 of Reinforcing Layer 1 and μ_2 of Subgrade Layer 2 on Vertical Stress Influence Coefficients, σ_z/p.

Figure No	Poisson's Ratio, μ Layer 1	Layer 2	Comparative Influences of Poisson's Ratio $r/h > 1.0$ Full Range of E_1/E_2	$r/h > 4.04$ $E_1/E_2 < 100$ at least
2	0.2 / 0.4	0.2] 0.2]	σ_z greater to 6 % σ_z^2 less	σ_z approaches 1.0 p Ditto
3	0.2 / 0.4	0.4] 0.4]	σ_z Greater to 6 % σ_z^2 less	$\sigma_z > 1.0$ p. $E_1/E_2 < 100$ Ditto

$$E_1/E_2 < 500, \quad \sigma_z/p > 0.6$$

4	0.2] 0.2]	0.2 / 0.4	σ_z less σ_z^2 greater to 2%	σ_z approaches 1.0 p $\sigma_z^2 > 1.0$ p
5	0.4] 0.4]	0.2 / 0.4	σ_z less σ_z^2 greater to 2%	σ_z approaches 1.0 p $\sigma_z^2 > 1.0$ p

It is to be noted in Fig. 3 that a Poisson's ratio of 0.4 in layer 2 for values of both 0.2 and 0.4 in layer 1 causes the vertical stress influence coefficient, σ_z/p to exceed 1.0 p, the surface loading. This means that the vertical stress must change to tension across the interface 1-2 over some portion of the interface outside of the limits of the loaded area beyond r/h of 6.0. Also a Poisson's ratio of 0.4 in layer 2 for values of both 0.2 and 0.4 in layer 1 causes the vertical stress influence coefficient in Figs. 4 and 5 to be greater. On the other hand a Poisson's ratio of 0.4 in layer 1 in Figs. 2 and 3 for both 0.2 and 0.4 in layer 2 causes the vertical stress, σ_z to be smaller. These figures disclose that Poisson's ratio does have significant and systematic influences on vertical stress intensities and distributions. Therefore, representative values of Poisson's ratio should be established for use in layered sys-

tem evaluations and investigations by laboratory and field experiments.

The magnitude and distribution of vertical stresses imposed with depth in layer 1 and layer 2 by surface loadings on a two layer system are shown in the following figures, and they disclose more completely the nature of vertical stress performances and effectiveness of reinforcing action, as governed by the basic two layer parameters- E_1/E_2, (μ_1, μ_2), r/h and z/h:

Table 4. Coverage of Figures for Vertical Stress Influence Coefficients, σ_z/p with Regard to Depth and Poisson's Ratio.

Figure No	Layer No	Depth- z/h	Full Line Curves μ_1	μ_2	Dotted Line Curves μ_1	μ_2
6	1	$\frac{1}{2}$	0.2	0.2	0.2	0.4
2	Interface 1-2	1	0.2	0.2	0.4	0.2
3	Interface 1-2	1	0.2	0.4	0.4	0.4
4	Interface 1-2	1	0.2	0.2	0.2	0.4
5	Interface 1-2	1	0.4	0.2	0.4	0.4
7	2	3/2	0.2	0.2	0.2	0.4
8	2	2	0.2	0.2	0.2	0.4
9	2	3	0.2	0.2	0.2	0.4
10	2	5	0.2	0.2	0.2	0.4

The curves of these figures represent the vertical stress influences imposed on the center line at depths, z = [z/h]h, noted in each figure beneath a surface loading uniformly distributed

-28-

Vertical Stress Influence Coefficient. σ_z/p beneath Center of Uniformly loaded Circular Area

FIG. 6 TWO LAYER VERTICAL STRESS INFLUENCE CURVES

σ_z/p Versus r/h at z = h/2

—————— (1) μ_1 = 0.2 μ_2 = 0.2
— · — · — (3) μ_1 = 0.2 μ_2 = 0.4

Vertical Stress Influence Coefficient, σ_z/p beneath Center of Uniformly Loaded Circular Areas

Values of Two Layer Parameter - r/h

FIG. 7 TWO LAYER VERTICAL STRESS INFLUENCE CURVES

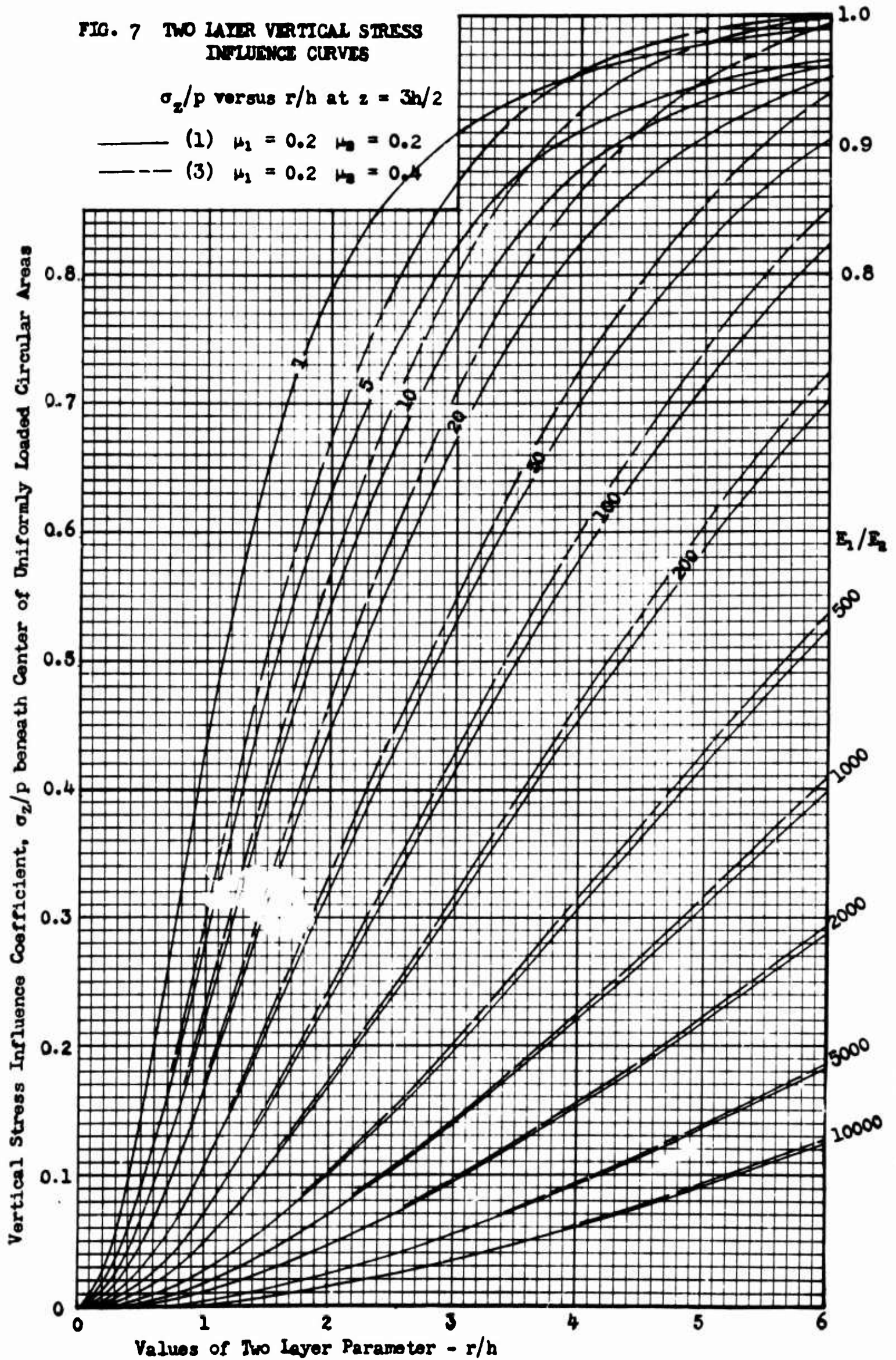σ_z/p versus r/h at $z = 3h/2$

——— (1) $\mu_1 = 0.2$ $\mu_3 = 0.2$

—·—·— (3) $\mu_1 = 0.2$ $\mu_3 = 0.4$

Vertical Stress Influence Coefficient, σ_z/p beneath Center of Uniformly Loaded Circular Areas

Values of Two Layer Parameter - r/h

E_1/E_2

FIG. 8 TWO LAYER VERTICAL STRESS
INFLUENCE CURVES

σ_z/p versus r/h at $z = 2h$

——— (1) $\mu_1 = 0.2$ $\mu_2 = 0.2$
—·—·— (3) $\mu_1 = 0.2$ $\mu_2 = 0.4$

Vertical Stress Influence Coefficient, σ_z/p beneath Center of Uniformly Loaded Circular Areas

Values of Two Layer Parameter - r/h

E_1/E_2

-31

FIG. 9 TWO LAYER VERTICAL STRESS INFLUENCE CURVES

σ_z/p versus r/h at $z = 3h$

——— (1) $\mu_1 = 0.2$ $\mu_2 = 0.2$

—·—·— (3) $\mu_1 = 0.2$ $\mu_2 = 0.4$

Vertical Stress Influence Coefficient, σ_z/p beneath Center of Uniformly Loaded Circular Areas

Values of Two Layer Parameter - r/h

E_1/E_2

FIG. 10 TWO LAYER VERTICAL STRESS INFLUENCE CURVES

σ_z/p versus r/h at $z = 5h$

——— (1) $\mu_1 = 0.2$ $\mu_2 = 0.2$
—·— (3) $\mu_1 = 0.2$ $\mu_2 = 0.4$

Vertical Stress Influence Coefficient, σ_z/p beneath Center of Uniformly Loaded Circular Areas

Values of Two Layer Parameter - r/h

E_1/E_2

over circular areas for increasing radius, $r = [r/h]h$. The
influence curves for each figure, plotting the vertical stress
influence coefficient, σ_z/p against the parameter, r/h are
referenced to the Boussinesq case for an homogeneous soil de-
posit with $E_1/E_2 = 1.0$ at the same depth, $z = [z/h]h$ in r/z.
It is to be noted especially in each figure that the family of
curves for E_1/E_2 increasing by regular steps from 1.0 to 50,000
form a systematic and consistent pattern characteristic for
each depth in the layered system.

The pattern of vertical stress influence curves in Fig. 6
for $z/h = 0.5$ at the mid-depth of reinforcing layer 1 exhibit
certain unusual aspects, which are, however, systematic and
consistent with increase in E_1/E_2 and are characteristic of
the vertical stress performances in reinforcing layer 1 of a
two layer system. These characteristics markedly influence
the shear stress distributions in layers 1 and 2 in a two layer
system. The vertical stress influences at the mid-depth of
layer 1 fall only slightly below the Boussinesq values for
r/h less than 0.5. For r/h greater than 0.5 the curves fan
out with increase in E_1/E_2, but they do not fall below $\sigma_z/p = 0.5$
for $E_1/E_2 = 50,000$.

The vertical stress influence curves for $z/h = 1$, 3/2, 2,3,
and 5 in Figs. 2 to 5, 7, 8, 9, and 10 fan out systematically
with increase in E_1/E_2 and r/h, but with increasing depth, z/h
in layer 2 they shift to correspondingly lower σ_z/p values,
which are referenced to the Boussinesq case at the same depth
with $E_1/E_2 = 1.0$. These influence curves disclose the effective-
ness of the reinforcing action by the marked vertical stress re-
ducing capacity of reinforcing layer 1 on stresses imposed in
layer 2 with increase in E_1/E_2. They also show that the effec-
tiveness of a two layer system decreases with increase in r/h,

either increasing r for constant h, or decreasing h for constant r, as shown by increasing σ_z/p value along each influence curve. These essential stress performances of a two layer system have important implications in design of pavement systems and on the effectiveness of a given pavement system with change in use to larger tire sizes and higher tire pressures.

Figures 4, 7, 8, 9, and 10 bring out clearly the nature and regions in layer 2 of significant influences of Poisson's ratio, μ in the combinations of Eq. (3) for layers 1 and 2. In layer 2, the dotted-line curves for $\mu_1 = 0.2$ and $\mu_2 = \underline{0.4}$ always yield significantly higher vertical stress influence co-efficients, σ_z/p in certain r/h and E_1/E_2 regions than the full-line curves for $\mu_1 = 0.2$ and $\mu_2 = \underline{0.2}$, which shows the influences of increase in Poisson's ratio from 0.2 to 0.4 in layer 2 for a constant value of 0.2 in layer 1. The percentage increase in σ_z/p for full-line curves is practically independent of r/h, decreases with increase in E_1/E_2 and increases with increase in z/h, as shown in Table 5(a). On the other hand, an increase in Poisson's ratio from 0.2 to 0.4 in layer 1 for constant values of 0.2 or 0.4 in layer 2 (figures not shown) causes a significant percentage decrease in values of σ_z/p, being practically inde-pendent of z/h, decreasing with increase in r/h, but increasing with E_1/E_2, as shown in Table 5(b). Hence, Poisson's ratio does have significant influences on the reinforcing action of layer 1.

Table 5. Significant Influences of Poisson's Ratio, μ_1 in Reinforcing Layer 1 and μ_2 in Subgrade Layer 2 for Vertical Stress Influence Coefficients at Interface 1-2.

a) Order of percentage increase in σ_z/p for dotted-line curves with $\mu_1 = 0.2$ and $\mu_2 = 0.4$ over full-line curves with $\mu_1 = 0.2$ and $\mu_2 = 0.2$, with increases in E_1/E_2 and z/h, but practically independent of r/h.

z/h E_1/E_2	5	10	20	50	100	200	500	1000	2000	5000	10,000
1	2	2	2	1	1	1					
3/2	6	5	5	3	3	2	2	1	1		
2	8	8	6	6	6	5	4	3	3	3	1
3	11	11	11	10	10	8	7	6	5	5	4
5	14	14	14	13	13	13	12	10	10	8	8

b) Order of percentage decrease in σ_z/p for increase in Poisson's ratio from 0.2 to 0.4 in layer 1 with constant values of 0.2 or 0.4 in layer 2 with increases in E_1/E_2 and r/h, but practically independent of z/h.

r/h E_1/E_2	5	10	20	50	100	200	500	1000	2000	5000	10,000
0.6	5	5	6	7	7	8	8				
1	5	5	6	6	7	7	8	8	8	8	
2	3	4	4	5	6	6	7	8	8	8	8
3	3	3	3	4	5	6	7	7	8	8	8
5	2	2	2	2	3	4	5	6	7	7	7

SHEAR STRESS INFLUENCE CURVES
$$\tau_{rz}/p \quad vs \quad r/h \text{ and } E_1/E_2$$

The character, magnitude, and distribution of shear stresses, τ_{rz} imposed by wheel loads in layers 1 and 2 of a two layer system are also of principal concern, because they make it possible to delineate regions of possible critical shear stresses at different locations with respect to single and dual wheel loadings or landing gear loadings applied on a pavement surface. The regions of high shear stresses, which exceed some adverse critical values with respect to mobilizable shear strengths, may become the most vulnerable regions of excessive shear deformations and hence of final breakdown of a layered pavement structure. It therefore becomes of major importance to evaluate such critical shear stress conditions.

A series of shear stress performance ratings have been plotted in Figs. 11, 12, and 13 to disclose the fundamental shear stress transmission characteristics and shear stress performances of two layer systems, as governed by the basic two layer parameters - E_1/E_2, (μ_1, μ_2), r/h and z/h. In Fig. 11 shear stress influence coefficients, τ_{rz}/p at the critical mid-depth of reinforcing layer 1 for z = h/2 are plotted against the parameter, r/h increasing from 0 to 6, and they form a systematic and characteristic family of influence curves for the full range of E_1/E_2 from 1.0 (Boussinesq case) to 50,000. Dotted-line curves are for Poisson's ratio - μ_1 = 0.2 and μ_2= 0.4, and the full-line curves for μ_1 = 0.2 and μ_2 = 0.2. It is most important to note the marked and adverse increase in shear stress influence coefficients at z = h/2 with increase in E_1/E_2 and also with increase in r/h, either increase in radius, r of

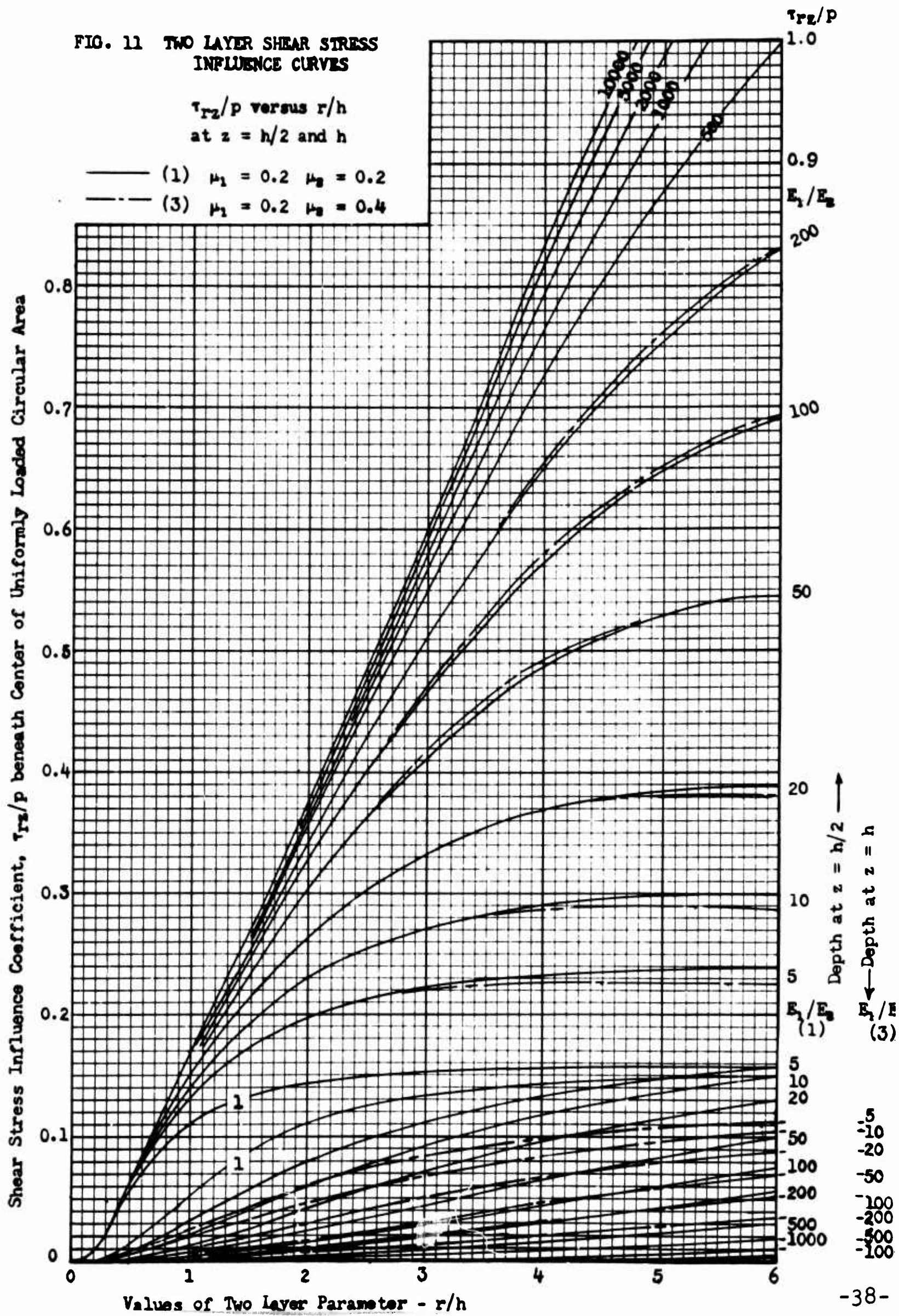-37-

FIG. 11 TWO LAYER SHEAR STRESS
INFLUENCE CURVES

τ_{rz}/p versus r/h

at $z = h/2$ and h

—————— (1) $\mu_1 = 0.2$ $\mu_2 = 0.2$

— · — · — (3) $\mu_1 = 0.2$ $\mu_2 = 0.4$

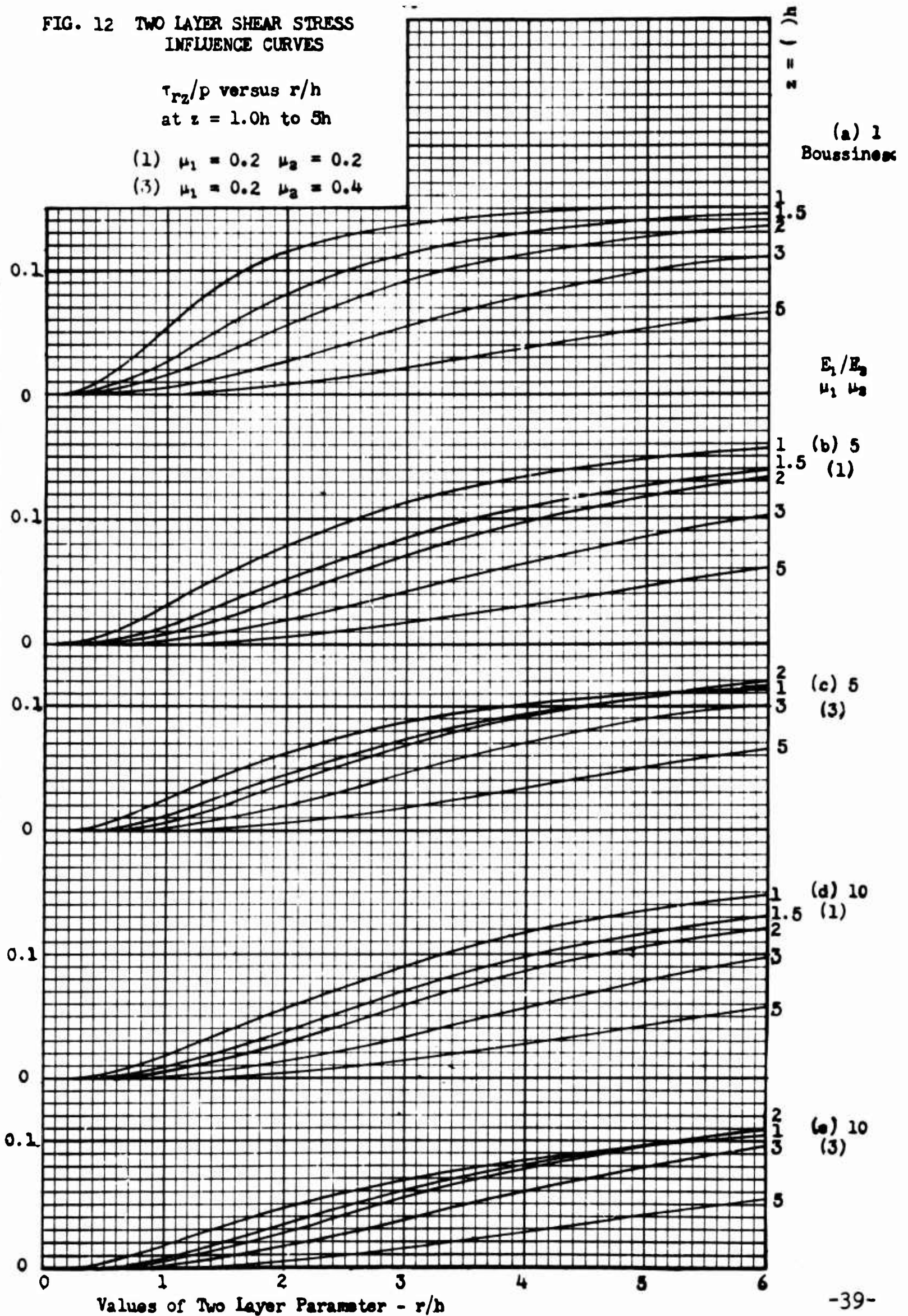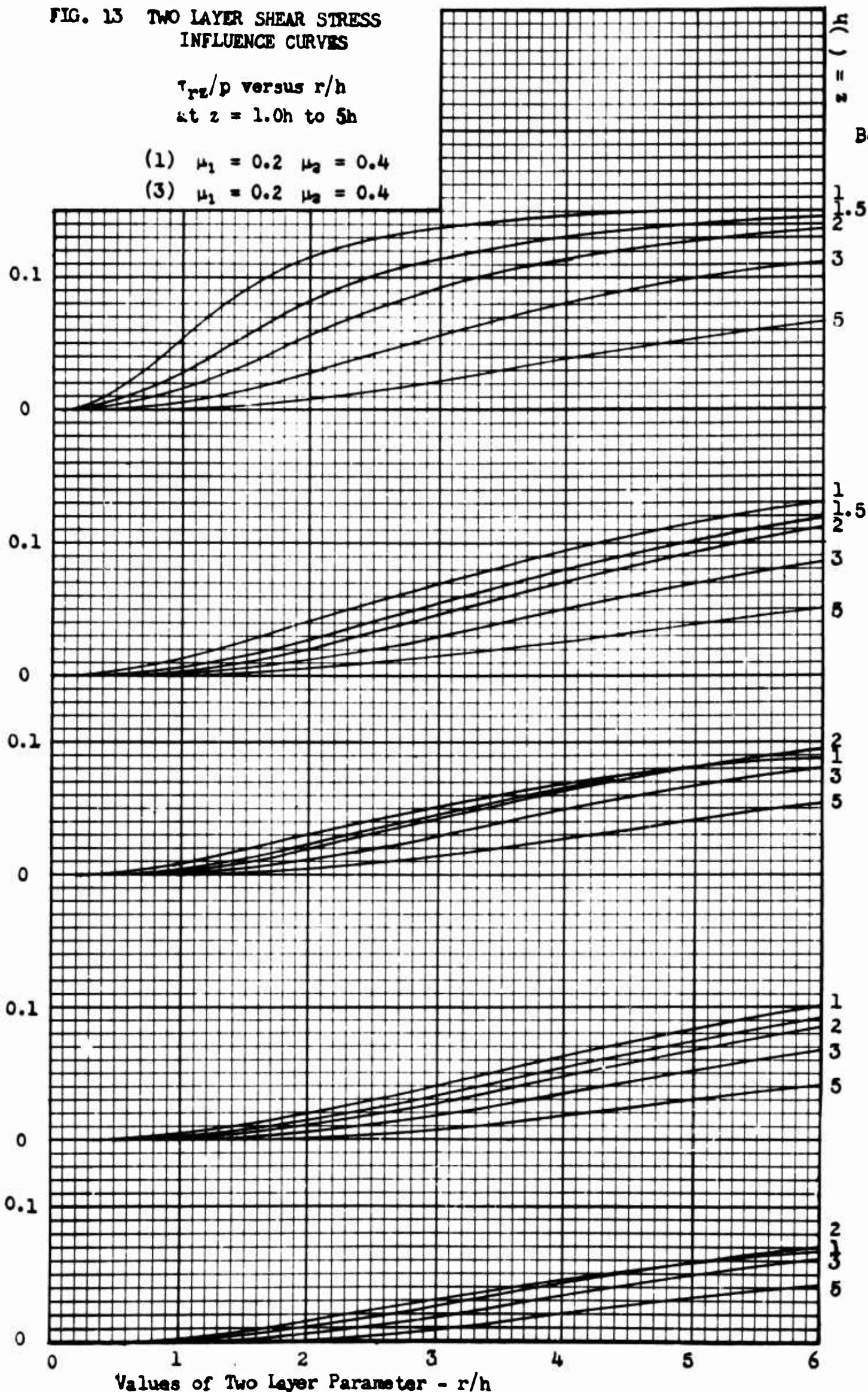Shear Stress Influence Coefficient, τ_{rz}/p beneath Center of Uniformly Loaded Circular Area

Values of Two Layer Parameter - r/h

-38-

FIG. 12 TWO LAYER SHEAR STRESS INFLUENCE CURVES

τ_{rz}/p versus r/h

at $z = 1.0h$ to $5h$

(1) $\mu_1 = 0.2$ $\mu_2 = 0.2$

(3) $\mu_1 = 0.2$ $\mu_2 = 0.4$

Shear Stress Influence Coefficient, τ_{rz}/p beneath Center of Uniformly Loaded Circular Area

Values of Two Layer Parameter - r/h

-39-

FIG. 13 TWO LAYER SHEAR STRESS
INFLUENCE CURVES

τ_{rz}/p versus r/h
at $z = 1.0h$ to $5h$

(1) $\mu_1 = 0.2$ $\mu_2 = 0.4$
(3) $\mu_1 = 0.2$ $\mu_2 = 0.4$

Shear Stress Influence Coefficient, τ_{rz}/p beneath Center of Uniformly Loaded Circular Area

Values of Two Layer Parameter - r/h

bearing area for constant thickness, h of reinforcing layer 1, or decrease in thickness, h for constant radius, r.

It is however, important to note in the lower portion of Fig. 11 that there is a marked and favorable decrease in shear stresses at the interface 1-2 between layer 1 and layer 2 with increase in E_1/E_2. The reinforcing action of layer 1 is favorably active in reducing the shear stresses imposed on the subgrade layer 2 below the Boussinesq reference values for a uniform soil deposit. Hence shear stresses become less critical in subgrade layer 2. Therefore, as long as the reinforcing action and competence of layer 1 are fully active, the shear stresses in the weaker subgrade layer 2 just on the underside of the interface 1-2 can not become critical unless these shear stresses at $z = 1.0h$ exceed the mobizable, sustained shear strength of the subgrade layer 2 material.

The maximum or peak shear stress influence coefficients occur at the following values of the parameter, r/h in Table 6, which greatly exceed the Boussinesq shear stress coefficient maximum of 0.157, as a reference in Fig. 11 at the same depth in an homogeneous soil deposit, $z = [r/h]h$ in r/z. It is to be noted especially that for increasing values of E_1/E_2 the curves depart more slowly from a basic envelope curve of shear stress influence coefficients for a two layer system.

Table 6. Maximum or Peak Shear Stress Influence Coefficients, τ_{rz}/p and associated r/h for a Two Layer System Versus the Parameter, r/h at Mid-Depth of Layer 1 for z = h/2.

E_1/E_2	$\mu_1 = 0.2$ $\mu_2 = 0.2$		$\mu_1 = 0.4$ $\mu_2 = 0.2$		$\mu_1 = 0.2$ $\mu_2 = 0.4$		$\mu_1 = 0.4$ $\mu_2 = 0.4$	
5	0.249	25.0	0.262	25.0	0.221	25.0	0.235	25.0
10	0.309	25.0	0.323	25.0	0.279	25.0	0.294	25.0
20	0.387	25.0	0.405	25.0	0.356	25.0	0.375	25.0
50	0.527	25.0	0.551	25.0	0.498	25.0	0.523	25.0
100	0.718	8.5	0.754	8.5	0.716	8.0	0.753	8.5
200	0.929	10.0	0.954	10.5	0.927	10.0	0.974	10.0
500	1.295	13.5	1.358	14.0	1.293	13.0	1.356	13.5
1000	1.657	16.5	1.735	16.5	1.654	16.5	1.734	17.0
2000	2.113	21.0	2.214	22.0	2.109	20.5	2.209	21.5
5000	2.856	23.0	2.990	24.0	2.883	25.5	3.004	25.0
10,000	3.507	25.0	3.627	25.0	3.505	25.5	3.620	25.0

It is evident in Fig. 11 that the influences of an increase in Poisson's ratio in layer 2 from 0.2 to 0.4 for a constant value of 0.2 in layer 2 on the shear stress influence coefficients is only moderately significant on a percentage bases for E_1/E_2 from 5 to 200 in the range of r/h greater than about 3.0. Also the influences of an increase in Poisson's ratio from 0.2 to 0.4 in layer 1 for constant values of 0.2 and 0.4, respectively, in layer 2 are only moderately significant on a percentage basis, being dependent principally on r/h for certain ranges of E_1/E_2, as shown in Table 7.

<u>Table 7.</u> Order of Influences of Poisson's Ratio, μ_1 in Reinforcing Layer 1 and μ_2 in Subgrade Layer 2, Expressed as a Percentage Increase in τ_{rz}/p in Fig. 11 at $z = h/2$ forIncrease in Poisson's Ratio from 0.2 to 0.4 in Layer 1 with Constant Values of 0.2 and 0.4, Respectively in Layer 2.

E_1/E_2 $r/h-$	1	2	3	5	7
5 to 50	1	2	3	4	5
100 to 500		1	2	3	2
1000 to 10,000			1	1	1

In Figs. 12 and 13 shear stress influence coefficients, τ_{rz}/p in layer 2 versus r/h are plotted at depths, z of 1.0h, 1 $\cdot$h, 2h, 3h and 5h. Influence curves for the Boussinesq case for $E_1/E_2 = 1.0$ are plotted in Figs. 12(a) and 13(a), as a reference. The following influence curves are paired for $\mu_1 = 0.2$ and $_2 = 0.2$, and $\mu_1 = 0.2$ and $\mu_2 = 0.4$ respectively: Figure 12(b) and (c) for $E_1/E_2 = 5$; Fig. 12(d) and (e) for $E_1/E_2 = 10$; Fig. 13(b) and (c) for $E_1/E_2 = 20$; and Fig. 13(d) and (e) for $E_1/E_2 = 50$.

It is evident from Figs. 12 and 13 that the reinforcing action of layer 1 is active in reducing shear stresses throughout layer 2, appreciably below the Boussinesq reference values in Figs. 12(a) and 13(a) for an homogeneous soil deposit, and they decrease rapidly with depth below the interface 1-2 between layers 1 and 2 for full range of E_1/E_2.

A comparison of paired curves of Fig. 12(b) and (c), Fig. 12(d) and (e), Fig. 13(a) and (b), and Fig. 13(a) and (d) shows that an increase in Poisson's ratio from 0.2 to 0.4 in

layer 2 causes an appreciable decrease in τ_{rz}/p for values of
z/h of 1, 1.5 and 2 over the range of r/h from 1.0 to 2.0.
For depths in layer 2 greater than z = 5h, the shear stress
influence coefficients become insignificant for E_1/E_2 greater
than 20 and for r/h less than about 3.0. The influences of
changes in Poisson's ratio in layer 1 for constant values in
layer 2 are appreciable at z = 1.0h on a percentage basis,
and are the reverse of the influences in layer 1 at z = h/2,
as shown in Table 8. In general the shear stresses and the
influences of Poisson's ratio become less significant with
depth in layer 2.

Table 8. Order of Influences of Poisson's Ratio, μ_1 in Rein-
forcing Layer 1 and μ_2 in Subgrade Layer 2, Expressed
as a Percentage Decrease in τ_{rz}/p in Figs. 12 and
13 at z = 1.0h for Increase in Poisson's Ratio from
0.2 to 0.4 in Layer 1 with Constant Values of 0.2
and 0.4, Respectively in Layer 2.

E_1/E_2 r/h	1	2	3	5	7
5 to 20		6	4	3	1
50 to 200		12	8	7	6
500 to 10,000		12	12	11	10

It is important to note in Figs. 12 and 13 with increase
in r/h above about 5.0, either increasing r for constant h, or
decreasing h for constant r that the shear stresses increase
and approach the Boussinesq shear stress values of Figs. 12(a)
and 13(a) at the respective depths, z = ( )h. This stress
phenomena is associated with the increasing adverse reduction
in effectiveness of reinforcing action of layer 1 with increase

in r/h. Also it is most important to note that any tendencies for excessive shear deformation in reinforcing layer 1 caused by excessive shear stresses of Fig. 11 would inevitably result in breakdown tendencies of effective reinforcing action in a layered system. This would reduce adversely the E_1/E_2 value. Hence the shear stresses in subgrade layer 2 would approach the higher Boussinesq values, as maximum, at all depths for any r/h value.

DEFLECTION INFLUENCE CURVES

$$F_w \quad vs \quad h/r \quad and \quad E_1/E_2$$

Thorough knowledge and understanding of, and clear insight into the character and importance of deflection performances and the controlling influences of the reinforcing action of two layer systems are essential for airfield pavement studies. evaluations, and designs. Two approaches have been used: In the emperical approach interpretations and evaluations of experimental data have been made and are possible only on an emperical and statistical base. Because the emperical approach can deal only with actual physically measured quantities. the scrength properties of the component layers and the effectiveness of reinforcing action of the layered system, as a structural unit, can not be evaluated quantitively. This is the principal limitation of the emperical approach.

In the theoretical experimental approach interpretations and evaluations of stress transmission performances. deflection performances, and effectiveness of reinforcing action are guided by theoretical considerations involving parametric relations. Only in the theoretical-experimental approach can the governing parameters and significant, valid, and practical parametric relations be developed, thoroghly tested, and established among the basic two layer system parameters - E_1/E_2, (μ_1, μ_ε), r/h and z/h. Very elaborate, carefully controlled, and difficult field and laboratory investigations would be required to determine by direct experimentation the stress transmission characteristics and stress performances of layered pavement systems with sufficient accuracy and coverage to pro-

vide practical and adequate bases for interpretations, and
evaluations of such investigations would be difficult and
would be open to question regarding validity of applications,
because the presence of stress measuring devices placed in a
layered system would modify in an unknown manner and degree
the stresses measured. On the other hand, the deflection
performances of layered systems can be determined readily and
accurately by field plate load-bearing tests, as an adequate,
reliable, and practical basis for evaluations and designs of
layered pavement systems. The basic problems here are: first
to develope practical and reliable methods for performing pro-
totype plate load-bearing tests on layered systems [22] and
second, to develope, test out, and establish proper methods
and parametric relations for interpreting, evaluating, and
applying the results of such prototype load-bearing tests, as
bases for layered pavement system evaluations and designs.
The theoretical-experimental deflection approach and layered
system parametric relations permit the determination and eva-
luation of deflection performances, layered system strength
ratios, E_1/E_2, and effectiveness of layered system reinforcing
action. Then by Figs. 2 to 13 for stresses and Figs. 14 and
15 for deflections, the stress transmission characteristics,
the stress and deflection performances, and the effectiveness
of reinforcing action can be evaluated.

A series of deflection performance ratings have been plot-
ted from computed data in Figs. 14 and 15 to disclose layered
system action and deflection performances for two layer systems,
as governed by the basic two layer parameters, E_1/E_2, (μ_1, μ_2),
r/h, z/h, and the deflection Eq. (7). Deflection coefficients.
F_w at the surface of a two layer system for z/h = 0 are plotted
against the parameter, r/h increasing from 0 to 6 and they form

FIG. 14   TWO LAYER DEFLECTION INFLUENCE CURVES

F_w versus r/h

at Surface, z = 0

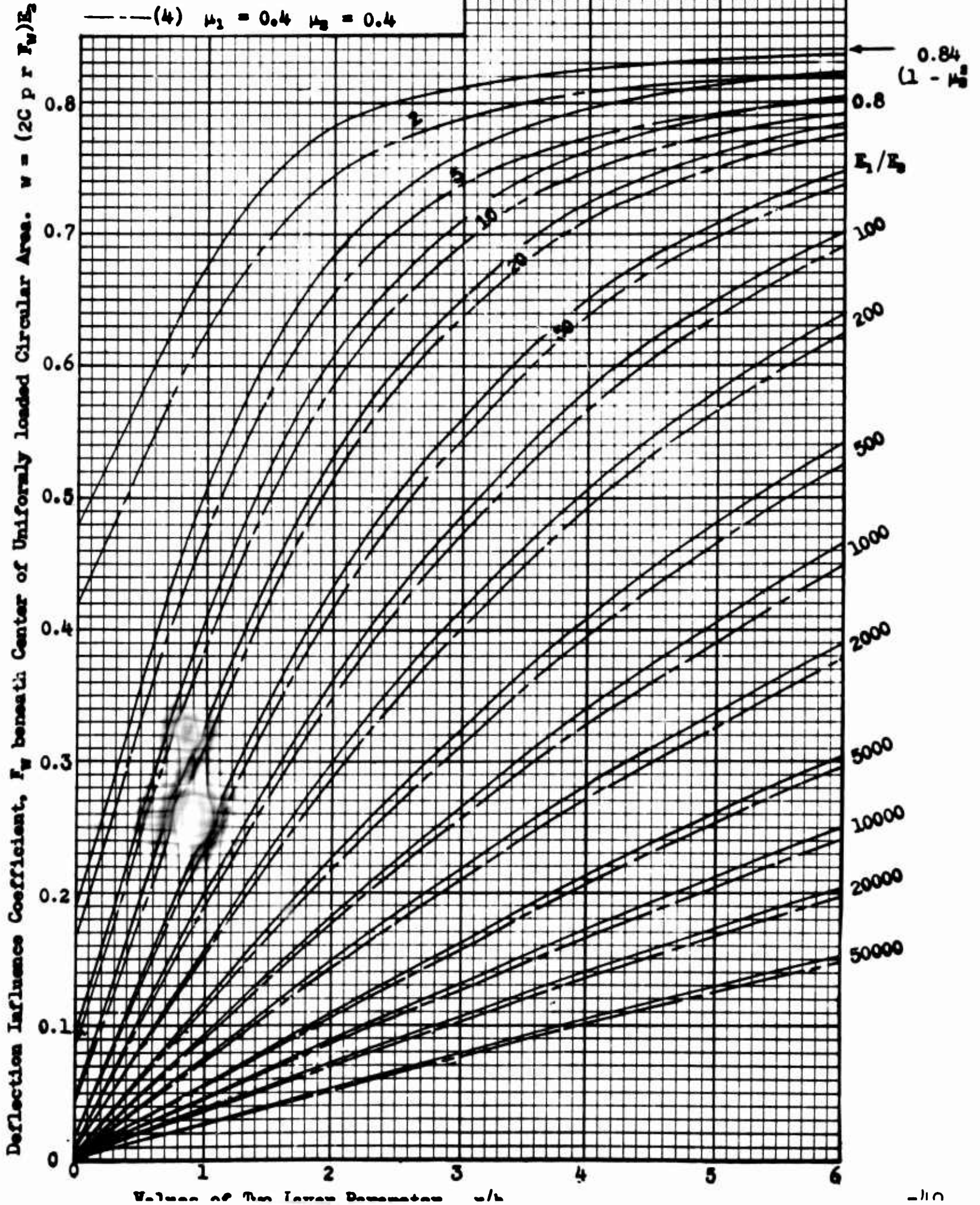(1) $\mu_1 = 0.2$ $\mu_2 = 0.2$
(2) $\mu_1 = 0.4$ $\mu_2 = 0.2$

For $E_1/E_2 = 1.0$ and r/h = ∞
$F_w = 1.0 \times (1 - \mu_2^2)$

FIG. 15 TWO LAYER DEFLECTION INFLUENCE CURVES

F_w versus r/h

at Surface, z = 0

———— (3) $\mu_1 = 0.2$ $\mu_2 = 0.4$

——·—— (4) $\mu_1 = 0.4$ $\mu_2 = 0.4$

For $E_1/E_2 = 1.0$ and $r/h = \infty$
$F_w = 1.0 \times (1 - \mu_2^2)$

0.84 $(1 - \mu_2^2)$

E_1/E_2

Deflection Influence Coefficient, F_w beneath Center of Uniformly loaded Circular Area. $w = (2C\, p\, r\, F_w)E_2$

Values of Two Layer Parameter, r/h

a systematic family of deflection influence curves for the full range of E_1/E_2 from 1 to 50,000. In Fig. 14 the full-line curves are for $\mu_1 = 0.2$ and $\mu_2 = 0.2$ and the dotted-line curves are for $\mu_1 = 0.4$ and $\mu_2 = 0.2$. The asymptotic value of F_w at $r/h = \infty$ is governed by Poisson's ratio, μ_2 in layer 2, being $(1 - 0.2^2) = 0.96$. In Fig. 15 the full-line curves are for $\mu_1 = 0.2$ and $\mu_2 = 0.4$ and the dotted-line curves are for $\mu_1 = 0.4$ and $\mu_2 = 0.4$. The asymptotic value of F_w at $r/h = \infty$ is governed by Poisson's ratio, μ_2 in layer 2, being $(1-0.4^2)=0.84$.

The marked increase in effectiveness of reinforcing action of layer 1 with increase in E_1/E_2 for constant values of r/h along vertical lines in Figs. 14 and 15 is disclosed by the marked reduction in the deflection coefficient, F_w and hence marked reduction and improvement in surface deflection performances at $z/h = 0$, as given by the layered system deflection equation - $w = (2C\ p\ r\ F_w)/E_2$. The stress reduction performances of σ_z/p in Figs. 2 to 5 at interface 1-2 for $z = h$ systematically follow the deflection reduction performances and reinforcing action of Figs. 14 and 15. These deflection performances are illustrated in Table 9 by decreasing values of F_w along horizontal lines for selected values of r/h. On the other hand, there is a considerable decrease in effectiveness of reinforcing action with increase in r/h along constant E_1/E_2 curves in Figs. 14 and 15, as illustrated by the increase in F_w, with increase in r/h in the vertical columns of Table 9. A comparison of stress performances in Table 1 and deflection performances in Table 9 brings out the systematic relationship of reinforcing action and similarity of patterns.

Table 9. Effectiveness of Reinforcing Action of Two Layer
Systems in Reducing Deflections, as Indicated by
Values of F_w at $z/h = 0$ versus E_1/E_2 and r/h for
$\mu_1 = 0.2$ and $\mu_2 = 0.4$ in Fig. 15.

Values of F_w for E_1/E_2

1	5	10	20	50	100	200	500	1000	2000	5000	10,000
0.5	0.364	0.263	0.196	0.137	0.106	0.083	0.060	0.048	0.038	0.028	0.022
1.0	0.507	0.407	0.329	0.247	0.162	0.159	0.118	0.094	0.075	0.055	0.044
1.5	0.612	0.521	0.440	0.345	0.283	0.230	0.172	0.139	0.111	0.082	0.065
2.0	0.684	0.606	0.529	0.429	0.359	0.296	0.225	0.182	0.146	0.109	0.087

Figures 14 and 15, Table 9, and deflection Eq. 7-$w=(2C\,p\,r\,F_w)/E_2$
show that the effectiveness of reinforcing action in reducing
surface deflections depends on the two layer parameters E_1/E_2 and
r/h, and on the contact bearing pressure, p. Increase in effec-
tiveness of a layered system may be achieved: (1) by use of
better quality and higher strength, E_1/E_2 materials in reinforc-
ing layer 1 for constant values of thickness, h of layer 1, of
radius, r of bearing area, and of contact bearing pressure, r
and p. Equivalent two layer systems with regard to reinforcing
action and deflection performances are indicated by some constant
selected deflection coefficient, F_w on horizontal lines in Figs. 14
and 15 by various E_1/E_2 and r/h combinations in Table 10. Equiv-
alent two layer systems with regard to deflection performances
could be obtained for constant radius of bearing area, r and con-
stant selected deflection coefficient, F_w by corresponding de-
creases in thickness, h of layer 1 for selected values of E_1/E_2.
However, increases in thickness, h of layer 1 for a constant
value of E_1/E_2 are required in order to reduce the deflection

coefficient, F_w and hence deflections. Compare equivalence of Tables 2 and 10.

Table 10. Equivalent Two Layer Systems with Regard to Deflection Performances and Reinforcing Action for $\mu_1 = 0.2$ and $\mu_2 = 0.4$, Indicated by E_1/E_2, F_w and r/h Combination from Fig. 15.

Values of r/h for E_1/E_2

F_w	5	10	20	50	100	200	500	1000
0.5	0.98	1.38	1.81	2.49	3.13	3.92	5.30	6.65
0.2	0	0.31	0.52	0.78	1.01	1.30	1.73	2.20
0.1	0	0	0.18	0.34	0.48	0.62	0.85	1.07

In order to bring out clearly regions of significant influences of Poisson's ratio in layeres 1 and 2 combination of μ_1 and μ_2 have been plotted in Figs. 14 and 15 for direct comparison. First of all, the asymptotic value of F_w is governed by μ_2 and is higher in Fig. 14 and equal to 0.96 (arrow) for $\mu_2 = 0.2$, than in Fig. 15 and equal to 0.84 (arrow) for $\mu_2 = 0.4$. In Fig. 14 an increase in μ_1 of layer 1 from 0.2 to 0.4 for a constant $\mu_2 = 0.2$ decreases the value of F_w and hence reduces deflections significantly over the entire range of E_1/E_2 and r/h given in the figure. Likewise in Fig. 15 an increase in μ_1 of layer 1 from 0.2 to 0.4 for C constant $\mu_2 = 0.4$ decreases the value of F_w and hence reduces deflections significantly over the entire range of E_1/E_2 and r/h given in the figure. These significant influences of Poisson's ratio on deflection performances in Figs. 14 and 15 are in accord and consistent with those of Figs. 2 and 3 and Table 3 for σ_z stress performances, as should be expected. The influences on effectiveness are similar.

The deflection performances (not shown here) of a two layer system at interface 1-2 for z = h show significantly lower deflections than at the surface for $z/h = 0$ for values of E_1/E_2 less than about 100 with μ, in the range of r/h of 0. to 6. This indicates that there is a significant elastic compression in reinforcing layer 1 in this range of E_1/E_2. For higher values of E_1/E_2 reinforcing layer 1 becomes relatively incompressible, but is deflected accordingly at top and bottom about equally, as indicated in Figs. 14 and 15.

VERTICAL STRESSES, SHEAR STRESSES AND SURFACE
DEFLECTIONS IN TWO LAYER SYSTEMS

The character, distribution and magnitude of vertical
stresses, shear stresses and surface deflections throughout
layers 1 and 2 of two layer systems are of principal concern
in evaluating their effectiveness and permanence of reinforc-
ing action and load spreading capacity, as a bases for judg-
ing the adequacy of design. When these are fully visualized
and known, their complex interacting influences become signif-
icant. It then is possible to delineate regions of critical
stress values in a two layer system and at locations with
respect to single and dual wheel or loanding gear loadings
applied on a pavement surface.

Vertical Stresses

The distribution and magnitude of vertical stresses be-
neath the center of a uniformly loaded circular area applied
on the surface of two layer systems are shown in Figs. 16 to
19, plotting σ_z/p versus z/r through layers 1 and 2, and form-
ing a systematic family of curves for values of E_1/E_2 increas-
ing by steps from 1.0 to 100. The Boussinesq case for a uni-
form soil deposit serves as a reference for comparison of ef-
fectiveness. The two layer parameter, r/h, which fixes the
ratio of the radius of loaded area to the thickness of reinforcing
layer 1, is held constant for each figure, being 2.0, 1.5, 1.0 and
0.5 for Figs. 16, 17, 18, and 19, respectively. For a constant
radius, r of bearing area, the thickness of reinforcing layer 1

FIG. 16 DISTRIBUTION OF VERTICAL STRESSES IN TWO LAYER SYSTEM
σ_z/p Versus z/r for $r/h = 2.0$
$\mu_1 = 0.2 \quad \mu_2 = 0.4$

FIG. 17 DISTRIBUTION OF VERTICAL STRESSES IN TWO LAYER SYSTEM
σ_z/p Versus z/r for $r/h = 1.5$
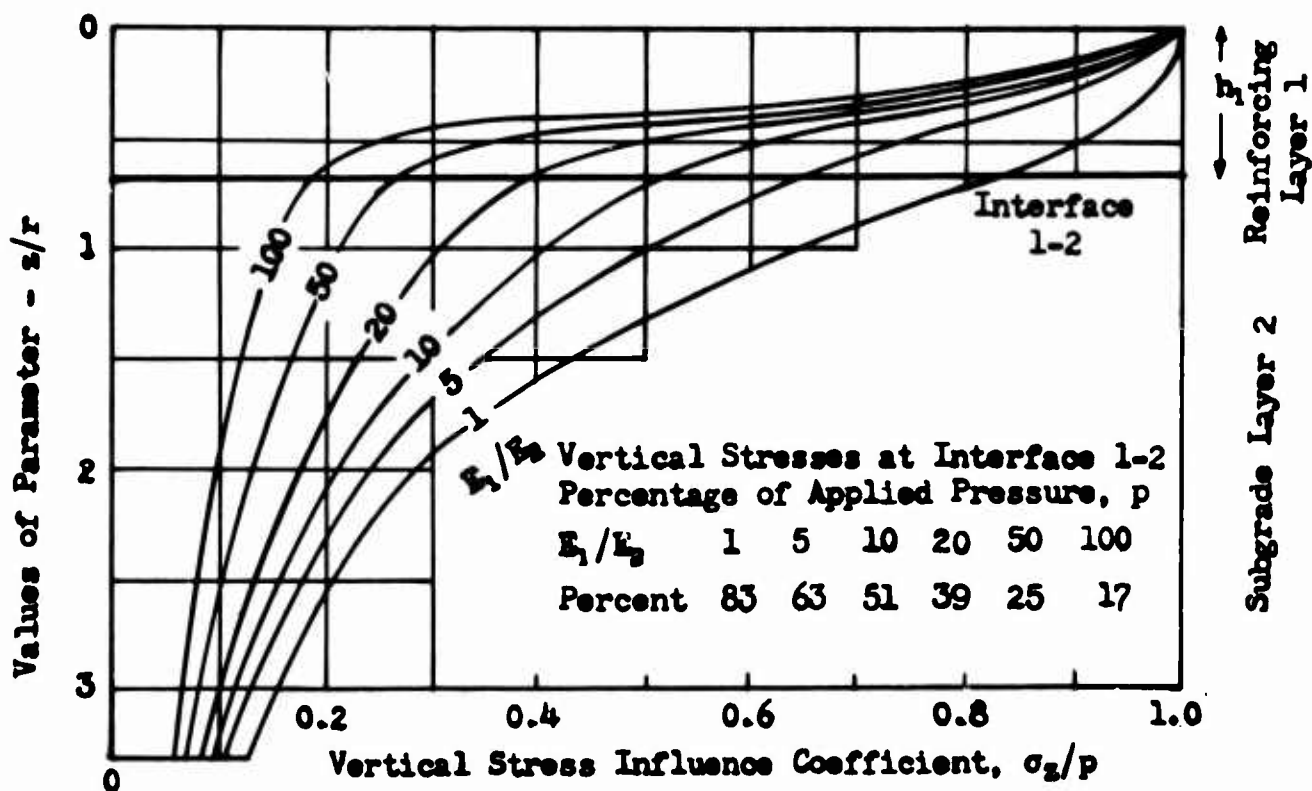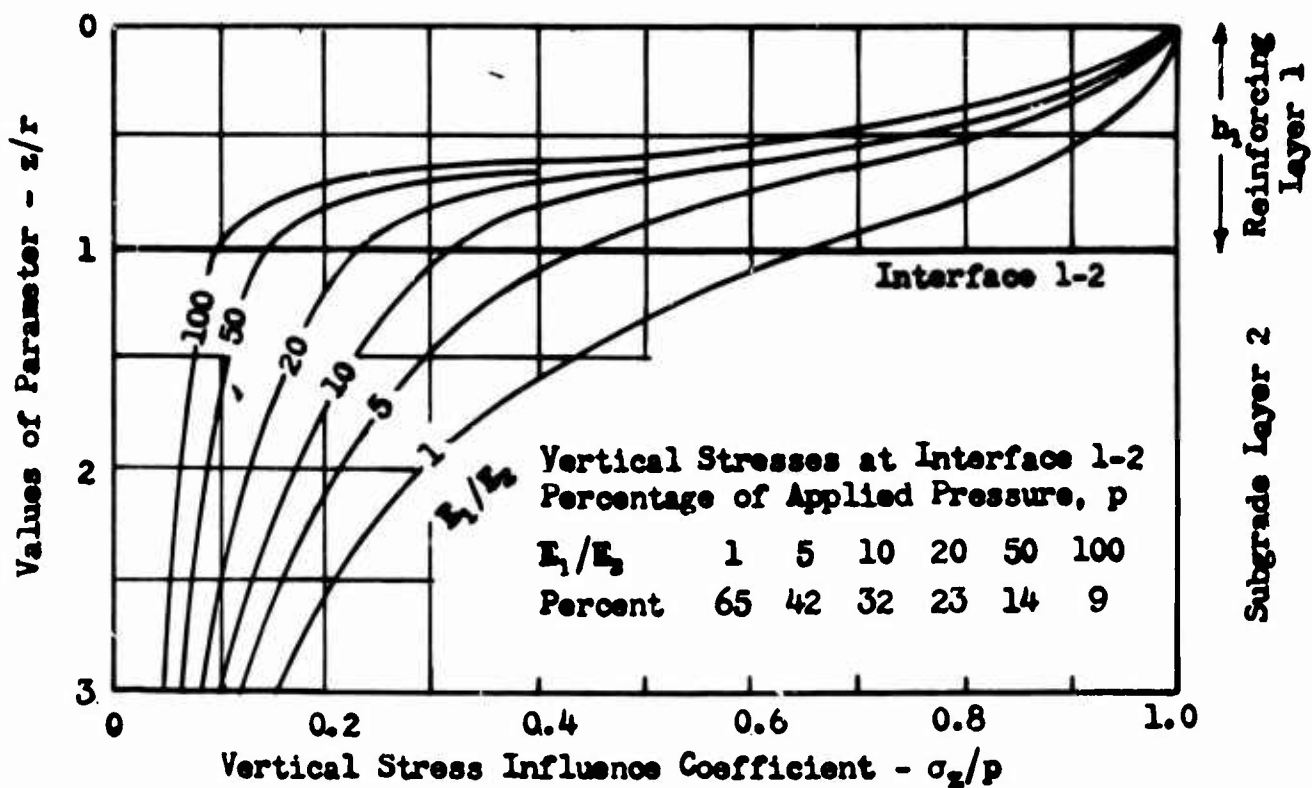$\mu_1 = 0.2 \quad \mu_2 = 0.4$

FIG. 18   DISTRIBUTION OF VERTICAL STRESSES IN TWO LAYER SYSTEM
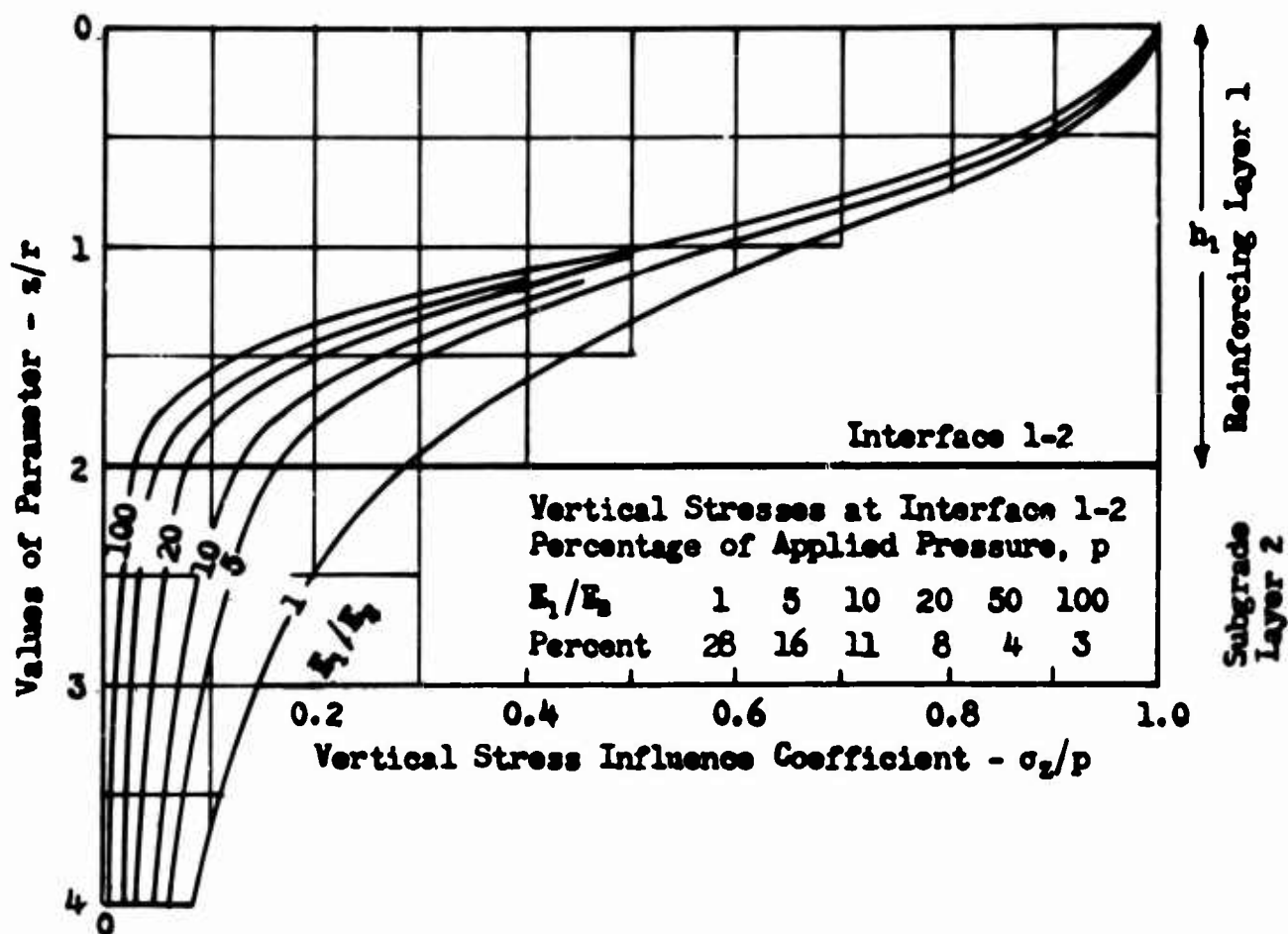σ_z/p Versus z/r for $r/h = 1.0$
$\mu_1 = 0.2$ $\mu_2 = 0.4$

FIG. 19   DISTRIBUTION OF VERTICAL STRESSES IN TWO LAYER SYSTEM
σ_z/p Versus z/r for $r/h = 0.5$
$\mu_1 = 0.2$ $\mu_2 = 0.4$

accordingly increases in these figures and has values of
$z/r = (z/h) \times 1/[r/h]$, or 1/2, 2/3, 1 and 2 respectively.
[3, Fig. 2, p. 3] [5, Fig. 2.p. 443].

These figures show that the character of vertical stres-
ses, the increase in effectiveness of reinforcing action, and
the favorable vertical stress reducing influences of layer 1
at interface 1-2 and with depth in subgrade layer 2 are gov-
erned by increases in the modulii strength ratio, E_1/E_2 and
by decreases in the parameter, r/h, either a relative increase
in thickness, h of layer 1 by decrease in radius of bearing
area, r, or by a physical increase in thickness, h for a con-
stant radius, r. The favorable vertical stress reduction at
interface 1-2 in protecting subgrade layer 2, expressed as
percentages of the applied bearing pressure, p, are given for
comparison in the table insert in each figure and they show
the marked influences of increase in E_1/E_2 and physical or
relative thickness of reinforcing layer 1 associated with de-
crease in the parameter, r/h. For a constant strength ratio,
E_1/E_2 the reinforcing action of layer 1 is most effective for
small r/h ratios, either decrease in radius of bearing area
for constant thickness, or increase in thickness for a constant
radius in Figs. 16 to 19. Conversely, for an increase in r/h
by increase in radius of bearing area, the reinforcing action
and vertical stress reducing influences of layer 1 of constant
thickness becomes less effective. The subgrade layer 2 then
assumes greater control over the stress transmission and deflec-
tion characteristics of a given layered system. It therefore
becomes clearly evident that the reinforcing action and vertical
stress reducing influeences of a given two layer system are not
constant, but are strongly and adversely influenced by increase
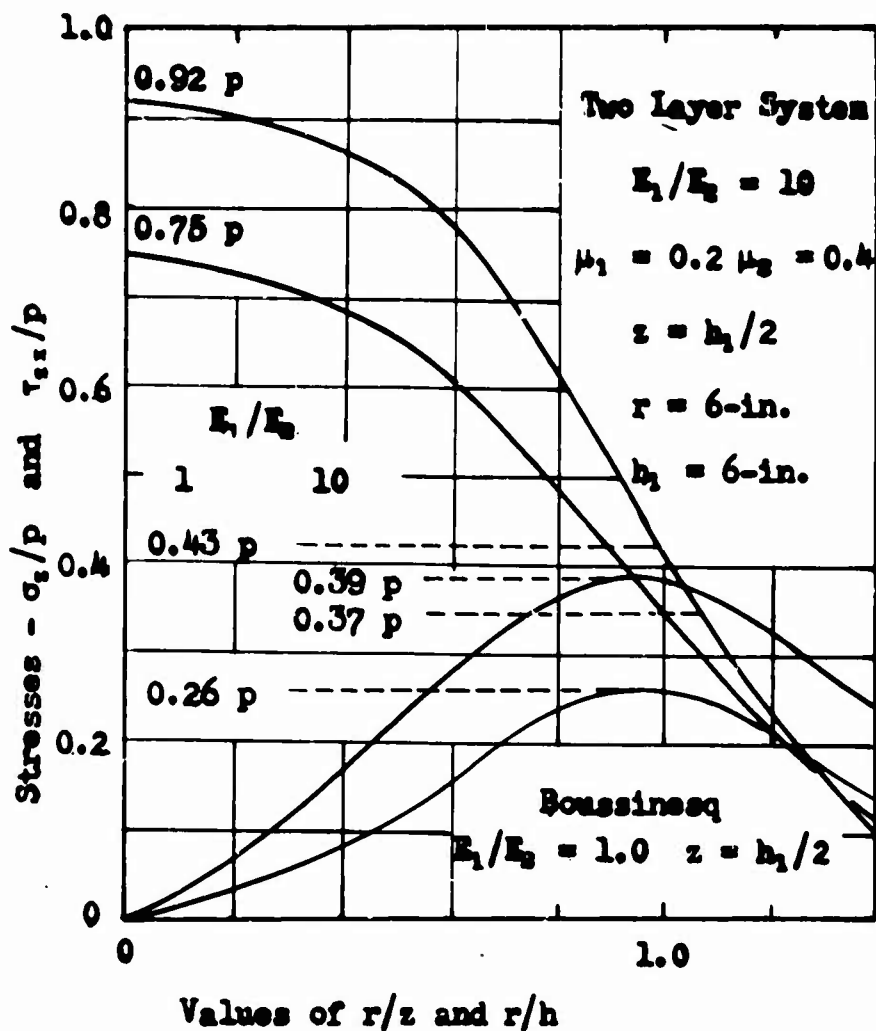in radius of bearing area through the two layer parameter, r/h.

These facts have important implications with regard to the effects of subsequent increase in radius and magnitude of wheel loadings, which a given pavement system may be called upon to support.
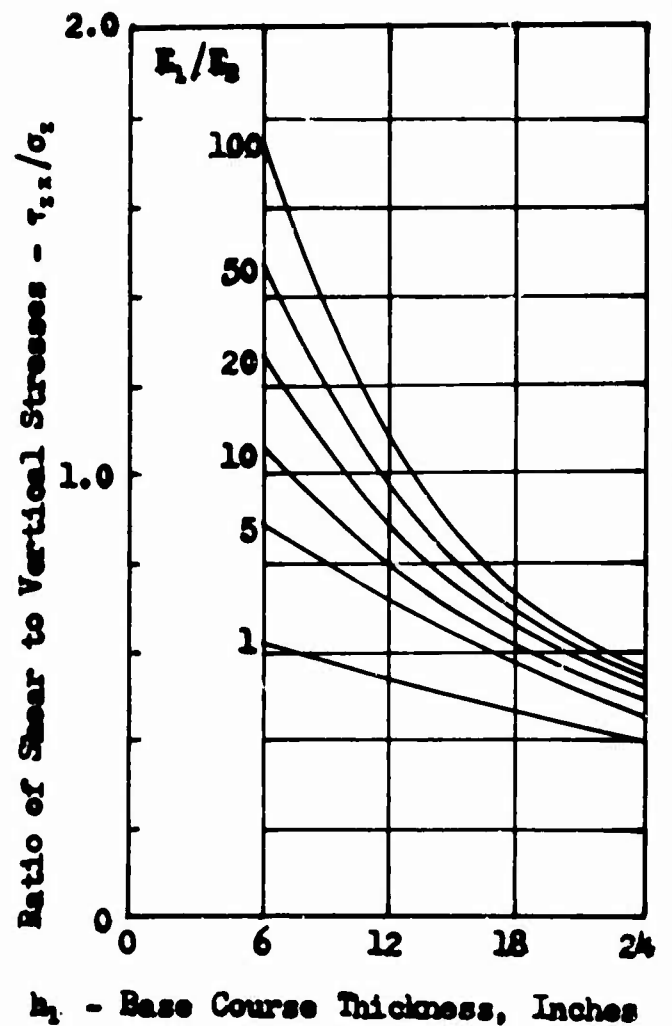
Shear Stresses

A most significant aspect of the vertical stress distributions in Figs. 16 to 19 is the marked vertical stress reduction and hence negative stress gradient, $-\partial\sigma_z/\partial z$ through reinforcing layer 1 with increase in E_1/E_2 in a two layer system. The only mechanism by which such a high negative vertical stress gradient can exist and can be maintained in a two layer system is by the presence of an equally high positive shear stress gradient and shear stress build-up through reinforcing layer 1 with increase in E_1/E_2 in accordance with the well-known stress equilibrium conditions of the theory of elasticity, expressed as stress gradients.

$$\frac{\partial\sigma_z}{\partial z} + \frac{\partial\tau_{rz}}{\partial r} + \frac{\tau_{rz}}{r} = 0 \qquad (16)$$
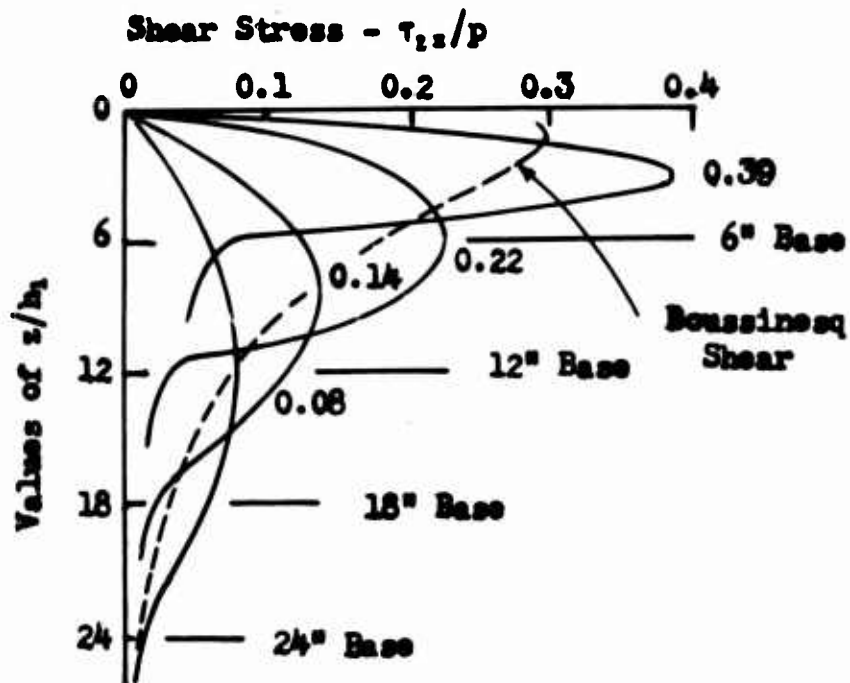
As a consequence of the increase in reinforcing action of layer 1 with increase in E_1/E_2 in a two layer system, the shear stresses in the reinforcing layer build-up and become more critical. The character and critical nature of the shear stresses in reinforcing layer 1 are illustrated in Fig. 20. The maximum shear stress in Fig. 20(a), which was obtained by special circular influence diagram and graphical integration methods for a uniformly loaded circular area, occurs in Fig. 20(a) beneath the edge of the circular area at $r/h = 1.0$ and in Fig. 20(b) at the mid-depth, $h/2$ of reinforcing layer 1 for $E_1/E_2 = 10$. The Boussinesq vertical stesses and shear
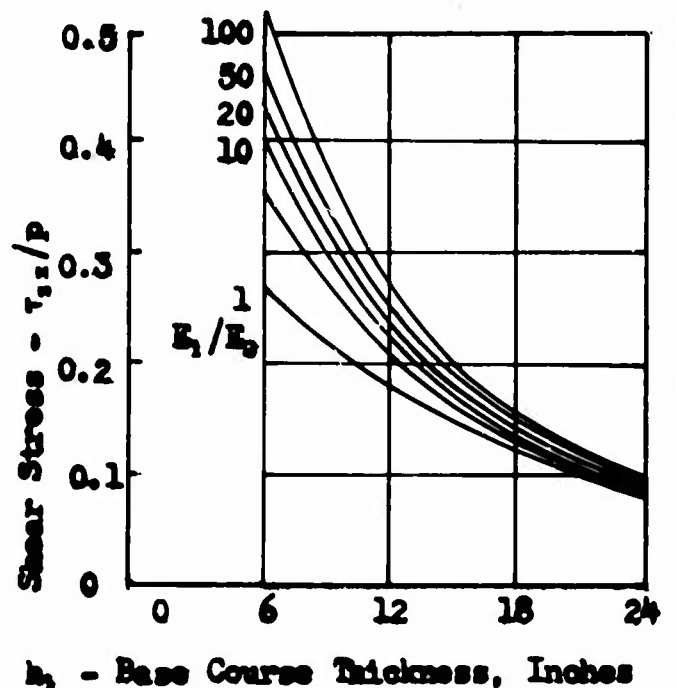
a) Evaluation of Two Layer System Vertical and Shear Stresses at Mid-depth of Layer 1 with regard to Critical Conditions in Comparison with Boussinesq Stresses

d) Ratio of Shear to Vertical Stresses Imposed at Mid-depth of Layer 1 beneath Edge of Bearing Area of Radius 6 Inches

b) Distribution and Magnitude of Shear Stresses Imposed in Layer 1 and Influences of Increased Thickness in Improving Conditions

e) Shear Stress Imposed at Mid-depth of Layer 1 beneath the Edge of Bearing Area of Radius 6 Inches

FIG. 20 CHARACTER, IMPORTANCE, AND CRITICAL NATURE OF SHEAR STRESSES IMPOSED IN REIN-FORCING LAYER 1 OF A TWO LAYER SYSTEM BENEATH THE EDGE OF A UNIFORMLY LOADED CIRCULAR BEARING AREA.

stresses for $E_1/E_2 = 1.0$ are given for comparison. The maximum shear stress, τ_{zx} for the two layer system in Fig. 20(a) imposed beneath the edge of the loaded circular area on the plane of the mid-depth of layer 1 is equal to 1.5 times the Boussinesq shear stress in an homogeneous soil deposit at this depth. [5, Fig. 3 p. 4-15].

Figure 20(b) illustrates the characteristic distribution of shear stresses through reinforcing layer 1 and the maximum shear stress at mid-depth, as a consequence of the stress gradient relations of Eq. (16). It is evident that shear stresses imposed at the mid-depth of layer 1 beneath the edge of a circular loaded area increase greatly and hence become more critical with decrease in thickness of reinforcing layer 1 for a constant 6-in. radius of bearing area and that they can be favorably reduced in intensity by increasing the thickness. Also it follows, that the shear stresses become more critical with increase in radius of loaded area for a constant thickness of layer 1. In Fig. 20(c) the controlling influences of E_1/E_2 on the maximum shear stresses imposed at mid-depth of layer 1 beneath the edge of a bearing area are illustrated. For the relatively thin 6-in. layer 1, the maximum shear stresses become much more critical in character with increase in E_1/E_2, but can be favorably reduced by increase in thickness of layer 1. It is evident that the mid-depth of layer 1 beneath the edge of a loaded circular area is the critical shear stress region of first importance in a two layer system. The shear stresses at the underside of interface 1-2 are much lower, but can, however, become critical if these shear stress magnitudes exceeding the mobilizable shear strength in the top of subgrade layer 2.

In Fig. 20(a) the maximum shear stress imposed at the critical mid-depth of layer 1 beneath the edge of a circular bearing area exceeds vertical stress at the same point in the ratio of τ_{zx}/σ_z = 0.39/0.37 = 1.05, whereas for the Boussinesq case at this same point, the ratio is only 0.26/0.43 = 0.61. This ratio, τ_{zx}/σ_z reveals more clearly the critical character of the maximum shear stresses in a two layer system, as shown in Fig. 20(d), the ratio increasing markedly and adversely with increase in E_1/E_2. Conditions can, however, be improved favorably by increasing the thickness of reinforcing layer 1. From the geometry conditions of layered systems with regard to radius of bearing area and thickness of reinforcing layer 1, Figs. 20(c) and 20(d) can be generalized for other radius-thickness combinations and conditions by using the associated r/h values noted in the figures.

C8 - As a consequence of the vertical stress and associated shear stress gradients of Eq. (16), the critical and adverse character of the shear stresses imposed at the critical mid-depth of reinforcing layer 1 beneath the edge of a loaded bearing area and of the ratio τ_{zx}/σ_z increases with increase in E_1/E_2 and r/h, either decrease in thickness, h for constant radius, r or increase in r for constant h, but decreases favorably with increase in thickness of reinforcing layer 1. C9 - The shear stress-strain and vertical stress-strain relations of Eq. (17), are as as follows:

$$\tau_{rz} = [\partial w/\partial r + \partial u/\partial z]E/(1 + \mu)$$

$$[\sigma_z - \mu\sigma_r - \mu\sigma_\theta] = E\partial w/\partial z$$

(17)

show clearly that the maximum shear stress imposed at the critical mid-epth of reinforcing layer 1 beneath the edge of a loaded

bearing area are essentially deflection-dependent. C10 - Shear stresses can not be imposed in reinforcing layer 1 without first of all having appreciable shear deformation in layer 1 caused by the deflection of the layered system under wheel loads, the quantity $\partial w / \partial r$ really representing the deflection curvature of the layered system under load.

These associated shear stress, vertical stress, and deflection relations in layered systems through concepts C1 through C10 give special point to the necessity of incorporating high prestress, mechanical bonding, and shear strength continuity throughout a layered system by the conditioning and prestressing influences of systematic heavy rolling. Such reinforcing base course and subbase layers are much superior in their deflection performances and supporting values, than would be the case if densified by vibration methods to the same relative densities, but without any prestressing and keying action by heavy rolling. But shear strength on the critical mid-depth plane can not be mobilized with out first of all having some slight shear deformations in reinforcing layer 1 (Eq. (7)) caused by deflection of a layered system under wheel loads. For granular base course and subbase materials of low coherence, the potential horizontal shear strength, S(max.) mobilizable by deflection on horizontal planes at the critical mid-depth of reinforcing layer 1 is given approximately by the following equation:

$$S(\text{max.}) = [\sigma_z + h\gamma/2 + p_N] \tan \phi / \text{F.S.} \geq \tau_{zx} \qquad (18)$$

where $h\gamma/2$ is the thickness of layer 1 times its unit weight above the critical mid-depth; σ_z is the imposed vertical stress on this plane; p_N is the effective influences of the

prestress, keying action, and shear strength continuity; τ_{zx} is the imposed shear stress on this plane; and F.S. is a suitable factor of safety to insure long life against a shear deformation breakdown of reinforcing layer 1. Base course and subbase materials of high quality and maximum compaction should possess an angle of friction, ϕ of 45° and greater. Figure 20(b), (c), and (d) indicate that in order to meet shear stress criteria and to limit shear deformations, the overall thickness of reinforcing layers 1 should be greater than 12 in. or in parametric values, r/h should be less than 0.5. It is fortunate, however, these figures show that shear stresses in the critical mid-depth region beneath the edge of a loaded bearing area decrease considerably in intensity with increase in thickness of the reinforcing layer 1.

The use of multi-layer pavement systems, increase in thickness of the effective combined reinforcing layers, and of smaller jumps in E_1/E_2, E_2/E_3, etc. values between layers provide the most effective and practical methods for controlling and limiting surface deflections, and hence for reducing shear stresses imposed in critical regions of layered systems to well below critical shear deformation breakdown values under the action of repeated wheel loadings sustained under traffic and service conditions. It is evident that the competence of layered systems depends on the permanence of reinforcing action of layer 1, which becomes in reality the criterion for adequacy of pavement system design. If actual breakdown of the reinforcing action of layer 1 and E_1/E_2 occurs by excessive shear deformation, then the shear stresses decrease in layer 1 and approach the lower Boussinesq values. This means that the shear stresses in the top of subgrade layer 1 must increase adversely toward the higher Boussinesq values and must become critical. The final phase of breakdown in this new critical region is due to excessive lateral

plastic displacements in the subgrade layer, which results in final local failure of a pavement system after effectiveness of reinforcing action and E_1/E_2 is lost.

Deflections

It is evident from the foregoing discussions of vertical stresses and shear stresses, that definite information on the character and intensity of vertical and shear stresses imposed by wheel loads in critical regions in layered pavement systems are indispensable for adequate design. Since shear stresses and shear strengths are deflection-dependent by Eqs. (17) and (18), the most satisfactory and practical method for the determination and evaluation on a factual numerical basis of significant system strength ratios, E_1/E_2 and stress-deflection performances performances is by field load-bearing tests. With this information available, estimates can then be made for all critical vertical and shear stresses by the layered system theory and stress influence curves.

The effectiveness of reinforcing action and the deflection performances of two layer systems were disclosed in the deflection influence curves of Figs. 14 and 15 by the value of the deflection coefficient, F_w, which depends on the basic two layer parameters, E_1/E_2 and h/r. For a constant r/h value, the deflection performances are markedly improved by increase in E_1/E_2, causing a favorable decrease in the value of F_w. But the critical shear stresses are increased thereby, as shown in Fig. 20. Effective improvement in deflection performances can be achieved by selection and use of high strength materials and particularly by actual constructional excellence in the field to attain the full potential strength properties, E_1/E_2 of these materials. The effectiveness of reinforcing action

and the deflection performances are strongly influenced by r/h values. For constant values of E_1/E_2 and of radius of bearing area, the greatest improvement in two layer system reinforcing action and deflection performances can be achieved by increase in thickness of layer 1 in the region of r/h less than 2.0, where the deflection influence curves are steepest. This is of fundamental importance as a practical and effective means for controlling and limiting shear stresses in the critical mid-depth region of layer 1 beneath the edge of a loaded bearing area. For r/h values greater than 2.0 the improvement of deflection performances with increase in thickness becomes less effective. Also it is important to note for a constant E_1/E_2 and thickness of reinforcing layer 1, that the effectiveness of layered system reinforcing action decreases considerably with increase in radius, r of the bearing area, and increase in r/h. This results in an adverse increase in the deflection coefficient, F_w, and is accompanied by an adverse increase in shear stresses in the critical region of layer 1, as indicated by an increase in r/h in Figs. 20(c) and (d). C11 - In view of the intimate interrelationships of shear stress and deflection performances, the deflection coefficient, F_w and deflection Eq. (7) provide practical and adequate criteria for evaluating the effectiveness of layered system reinforcing action, stress-deflection performances, and critical shear stresses, and for correcting and improving permanence of required performances for design purposes.

The essential and necessary design requirements and objectives are: (1) to limit accumulated pavement settlements under repeated wheel loadings to non-objectionable values; (2) to insure the permanence, integrity, and continuity of the pavement structure against shear failure in critical regions under

repeated wheel loads; and (3) to increase the life of the pavement structure, giving due consideration to scientific, practical, and economic aspects. Pavement design always deals with multi-layer systems. The design of a multi-layer pavement system adequately to satisfy these requirements involves: (1) a determination of the number of layers required to limit shear stresses imposed incritical regions to well below shear breakdown values by using smaller jumps in E_1/E_2 values between layers; (2) the selection of suitable layer materials and the determination of corresponding E-values in order to control and to limit deflections and permanent settlements; and (3) the evaluation of thickness requirements of these layers in order to attain the above objectives.

REFERENCES

Papers by Donald M. Burmister

1. The Theory of Stresses and Displacements in Layered Systems and Applications to the Design of Airport Runways. Proceedings of the Highway Research Board, Vol. 23, pp. 126-149, 1943.

2. The General Theory of Stresses and Displacements in Layered Systems. Journal of Applied Physics, Vol. 16, Nos. 2, 3, 5, 1945.

3. Evaluation of the Pavement Systems of the WASHO Road Test by Layered System Methods. Highway Research Board Bulletin 177, 1958.

4. Flexible Pavement Design for Airfields. Interim Report to The Navy Department, Bureau of Yards and Docks, Contract NBy-13009, May 12, 1961.

5. Applications of Layered System Concepts and Principles to Interpretations and Evaluations of Asphalt Pavement Performances and to Design and Construction. International Conference on Structural Design of Asphalt Pavements. University of Michigan, Ann Arbor, Michigan, pp. 441-453, Figs. 1 - 4, 1962.

6. Applications of Layered System Concepts to Design and Construction of Asphalt Pavement. Proceedings of First Paving Conference 1962, Civil Engineering Department, University of New Mexico, Albuquerque, New Mexico, pp. 147-184, Figs. 1 - 9.

7. Layered System Design as Applied to Concrete Pavements. Proceedings of Second Paving Conference 1963, Civil Engineering Department, University of New Mexico, Albuquerque, New Mexico, pp. 21-47, Figs. 1 - 8.

8. Judgment and Environmental Factors in Soil Investigations. ASTM Bulletin, October 1956, p. 56, American Society for Testing Materials.

9. Identification and Classification of Soils. ASTM Special Technical Publication No. 113, pp. 3-24, 1951.

10. Suggested Method of Test for Identification of Soils. Procedures for Testing Soils, pp. 199-211, American Society for Testing Materials, 1958.

References Continued - Papers by Donald M. Burmister

11. Importance and Practical Use of Relative Density in Soil Mechanics. Proceedings, American Society for Testing Materials, Vol. 48, pp. 1249-1268, 1948.

12. Suggested Method of Test for Maximum and Minimum Densities of Granular Soils. Procedures for Testing Soils, pp. 148-150, American Society for Testing Materials, 1958

13. Principles of Permeability Testing of Soils. ASTM Special Technical Publication No. 163, pp. 3-26, 1955.

14. Suggested Method of Test for Permeability of Granular Soils. Procedures for Testing Soils, pp. 239-254, American Society for Testing Materials, 1958.

15. The Applications of Controlled Test Methods to Consolidation Testing. ASTM Special Technical Publication No. 126, pp. 83-97. 1951.

16. Suggested Method of Test for Consolidation of Soils. Procedures for Testing Soils, pp. 287-296, American Society for Testing Materials, 1958.

17. The Importance of Natural Controlling Conditions upon Triaxial Test Conditions. ASTM Special Technical Publication No. 106, pp 248-266, 1951.

18. The Place of Direct Shear in Soil Mechanics. ASTM Special Technical Publication No. 131, pp. 3-18, 1953.

19. Applications of Environmental Testing of Soils. American Society for Testing Materials, Vol. 56, pp. 1351-1371, 1956.

20. Strain-Rate Behavior of Clay and Organic Soils. ASTM Special Technical Publication No. 254. pp. 88-105, 1959.

21. Physical, Stress-Strain, and Strength Responses of Granular Soils. ASTM Special Technical Publication No. 322, pp. 67-97, 1962.

22. Prototype Load Bearing Tests for Foundations of Structures and Pavements. ASTM Special Technical Publication No. 322, pp. 98-119, 1962.